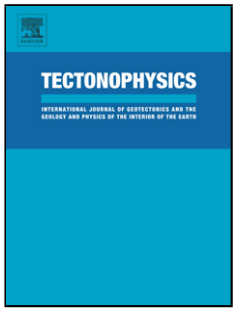

Inherited basement structures and their influence in foreland evolution: A case study in Central Patagonia, Argentina

Emiliano M. Renda, Dolores Alvarez, Claudia Prezzi, Sebastián Oriolo, Haroldo Vizán

PII: S0040-1951(19)30347-6

DOI: https://doi.org/10.1016/j.tecto.2019.228232

Reference: TECTO 228232

To appear in:

Received Date: 16 July 2019

Revised Date: 15 October 2019

Accepted Date: 18 October 2019

Please cite this article as: Renda EM, Alvarez D, Prezzi C, Oriolo S, Vizán H, Inherited basement structures and their influence in foreland evolution: A case study in Central Patagonia, Argentina, *Tectonophysics* (2019), doi: https://doi.org/10.1016/j.tecto.2019.228232

Inherited basement structures and their influence in foreland evolution: A case study in Central Patagonia, Argentina.

Emiliano M. Renda[a*], Dolores Alvarez[b], Claudia Prezzi[a], Sebastián Oriolo[a], Haroldo Vizán[a]

[a]CONICET-Universidad de Buenos Aires. Instituto de Geociencias Básicas, Aplicadas y Ambientales de Buenos Aires (IGEBA), Intendente Güiraldes 2160, C1428EHA Buenos Aires, Argentina

[b]SEGEMAR-Servicio Geológico Minero Argentino, San Martin, Provincia de Buenos Aires, Argentina.

[*]Corresponding author: Emiliano M. Renda

Email: renda.emi@gmail.com

Full Postal address: Intendente Güiraldes 2160, C1428EHA Buenos Aires, Argentina

Highlights

- Recurrent deformation and reactivation of faults that can be persistent for hundreds of millions of years

- In extra-andean Patagonia, we define a series of ~NW-SE regional structures which governed the present-day basement-block architecture of the foreland and exerted an important control in the deposition of Mesozoic-Cenozoic sedimentary and volcanic sequences
- The tectonic significance of these structures and their paleogeographic implications in the context of the Late Paleozoic Gondwanide magmatic arc are also discussed.

Abstract

Continental crust exhibits areas of recurrent deformation and reactivation of faults that can be persistent for hundreds of millions of years. Associated with weak lithospheric zones, the characterization of long-lived deformational zones and inherited structures are critical aspects in the construction of orogens and rift systems, playing a major role in magmatism and basin evolution. Central Patagonia, which is situated in the Andean foreland of southern South America, presents a complex and multi-episodic tectonic history related to intraplate deformation at a significant distance from the Andean trench. Its ~NW-SE structural trend, which is anomalously oblique to the Andean orogen, has been proposed as an inherited crustal anisotropy that controlled Mesozoic basins and Cenozoic volcano-sedimentary foreland basins development. However, a systematic regional study focused on the basement structural anisotropy has not been undertaken so far. In this contribution, we use aeromagnetic and gravimetric datasets that are integrated with field geological and structural data to address this issue. We define a series of ~NW-SE regional structures which governed the present-day basement-block architecture of the foreland and exerted

an important control in the deposition of Mesozoic-Cenozoic sedimentary and volcanic sequences. The tectonic significance of these structures and their paleogeographic implications in the context of the Late Paleozoic Gondwanide magmatic arc are also discussed.

Keywords: Structural Inheritance, Aeromagnetic survey, Gravimetry, Broken foreland, North Patagonia

1. Introduction

In relict orogenic zones, basement inherited structures exert a major structural control on the successive development of basins and reactivated faults (Sykes, 1978; Daly et al., 1989; Butler et al., 2006). These areas are considered as zones of lithospheric weakness, and strongly influence the development of orogenic belts, fault-controlled sedimentary basins, rift basins, intraplate deformation, volcanic activity and the channeling of ore-bearing fluids (Sykes, 1978; Daly et al., 1989; Marshak and Paulsen, 1996; Holdsworth, et al., 2001, Holdsworth, 2004; Tesauro et al., 2009; Fossen et al., 2016). In foreland settings, numerous provinces are characterized by uplift of fault-bounded basement blocks controlled by an inherited structural anisotropy, such as the Laramide Rocky Mountain Ranges in United States of America and the Sierras Pampeanas of Argentina (Jordan & Allmendinger, 1986; DeCelles, 2004; Şengör el al., 2018). Therefore, the characterization of long-lived deformational zones and the study of their inherited structures is a critical aspect in the analysis of crustal-scale tectonic processes.

The Patagonian broken foreland represents a contractional deformational zone related to the Andean orogeny (Folguera and Ramos, 2011; Bilmes et al., 2013; Gianni et al., 2015, 2017; Echaurren et al., 2016; Savignano et al., 2016; Navarrete et al., 2016; Bucher et al., 2019a, b). This

orogen is characterized as a thick-skinned fold and thrust belt, it occupies a zone of ~750 km of latitudinal extent and exhibits a NW-SE to NNW-SSE structural trend (Fig. 1). This area has been exposed to a long and recurrent tectonic history, which includes a possible Middle to Late Paleozoic continental collision or accretionary stage (Pankhurst et al., 2006; Ramos, 2008; Vizán et al., 2017), Late Triassic-Jurassic rifting processes (Uliana and Biddle, 1987; Figari, and Courtade, 1993; Figari, 2005), Cretaceous to Cenozoic fault reactivation and inversion (Dalla Salda and Franzese 1987; Figari, 2005; Bilmes et al., 2013; Gianni et al., 2015; Echaurren et al., 2016) and Cenozoic widespread basaltic magmatism (Folguera and Ramos, 2011).

The structural influence of basement inherited structures in this area has been previously suggested for the development of Jurassic-Cretaceous rift basins (Figari et al., 2015), the tectonic inversion of these faults and the Cenozoic fault-controlled uplift of basement blocks (Figari et al, 2015; Bilmes et al., 2013). However, most contributions have been mainly focused on the Mesozoic to Cenozoic tectonic and volcano-sedimentary processes, with little attention given to the Paleozoic basement structural fabric, even though this zone has been alternatively proposed as an active margin (Forsythe, 1982), a suture zone between two crustal blocks (Pankhurst et al., 2006; Ramos, 2008), an intracontinental large-scale dextral shear zone known as “Gastre fault system” (Rapela and Pankhurst, 1992) or as part of a weak lithospheric zone between Western and Eastern Gondwana (Vizán et al., 2017).

In this study, we recognize major-scale structures in the Patagonian broken foreland by means of aeromagnetic and global gravimetric data. We discuss the relationship of the Paleozoic inherited structural fabric with these structures considering field data, thus providing temporal constraints for basement anisotropy. We also analyze these results in the context of the Gondwanan margin

for Late Paleozoic times discussing the tectonic significance of these structures and its relationship with the subsequent Mesozoic to Cenozoic extensional and contractional deformation.

2. Geological Setting

The Extra-Andean Patagonia has been divided into two main morphostructural units, namely, the North Patagonian Massif and the Deseado Massif (Fig.1; Feruglio, 1949; Bracaccini, 1960). Our study area comprises the limit between both massifs, located in central Patagonia (Fig. 1), which is part of the Patagonian broken foreland (Folguera and Ramos, 2011). In this region, the distribution of Mesozoic and Cenozoic volcano-sedimentary units is strongly controlled by a regional NW-SE to-NNW-SSE structural fabric (Coira et al., 1975; Dalla Salda and Franzese 1987; Giacosa and Heredia 2004; Folguera and Ramos 2011; Orts et al., 2012; Bilmes et al. 2013; Gianni et al., 2015, 2017). In central Patagonia, outcrops of Devonian to Permian granitoids and associated metamorphic rocks are scattered, and are mostly covered by Mesozoic to Cenozoic volcano-sedimentary sequences (Fig. 1). This Paleozoic igneous belt is located immediately to the east of the back arc Early Missisipian-Cisuralian Tepuel-Genoa basin (Limarino and Spaletti, 2006).

2.1 Basement geology of the Patagonian broken foreland

The Paleozoic basement of the study area is mainly composed of metaluminous and peraluminous Devonian to Permian granitoids (Fig.1), which intrude metamorphic rocks ranging from greenschist to amphibolite facies (Dalla Salda et al., 1991, 1994; García-Sansegundo et al., 2009; Giacosa and Heredia, 2004; Martínez et al., 2012; Pankhurst et al.,

2006; Varela et al., 2005, 2015). In this work, this Paleozoic basement is collectively named the "Paleozoic Central Patagonian igneous-metamorphic belt" (Fig. 1).

This basement is well-exposed in the western and southwestern limit of the North Patagonian Massif, but is covered by younger units south of the Paso de Indios locality (Fig. 1). It is composed by medium- to high-grade schists, gneisses and minor quartzites of the Cushamen Formation (Volkheimer 1964, Dalla Salda et al., 1994; Giacosa et al., 2004). Several syn-deformational igneous bodies of tonalitic to granitic composition of the Mamil Choique Formation (Ravazzoli and Sessana, 1977) are concordant with the metamorphic foliation found in Cushamen Formation. The depositional age of the Cushamen Formation is constrained by U-Pb detrital zircon data, yielding a maximum deposition age of ~335 Ma (Fig. 1, Hervé et al., 2005). Along the Andean ranges, the equivalent metasedimentary unit is locally defined as the Colohuincul Formation (Turner, 1965). Monazite Th-U-Pb ages of ~392 and ~350 Ma in migmatites and schists of the Colohuincul Formation were reported (Fig. 1, Martinez et al, 2012), whereas monazite Th-U-Pb ages of ~302 and 299 Ma were also obtained for micaschists (Fig. 1, Oriolo et al., 2019). Comparably, zircon overgrowths in El Maiten Gneiss record late Devonian to middle Carboniferous amphibolite-facies metamorphism (Fig. 1, Pankhurst et al., 2006). Upper amphibolite facies metamorphism was also identified further east in the extra-Andean Patagonia, near Gastre (Fig. 1), where the pre-Devonian Caceres Complex is exposed (Giacosa et al., 2014).

Geochronological and geochemical data indicate the presence of Late Carboniferous to Late Permian I- and S-type granites, granodiorites and tonalites (Pankhurst et al., 2006; Varela et al., 2005; 2015), associated with the Cushamen and Colohuincul formations (Dalla Salda et al., 1994; Cerredo and López de Luchi, 1998; Giacosa et al, 2004; García-

Sansegundo et al., 2009; Oriolo et al., 2019). Drill cores in the San Jorge basin revealed the presence of granitoids with K-Ar Carboniferous ages (see Fig. 1, Linares and González, 1990). These igneous and metamorphic rocks cross this basin and continue through the Deseado Massif and can be traced further southeast, in the offshore, in the Punta Dúngenes high (Ramos, 2008).

2.2 Mesozoic-Cenozoic geology in Central Patagonia

Volcanic activity was widespread in Patagonia during the Early Jurassic, associated with the Western Gondwana break-up and the development of NNW-SSE rift systems (Uliana and Biddle, 1987). The syn-rift sedimentary successions of the Cañadon Asfalto Basin (CAB, Fig. 1) include voluminous volcanic and volcaniclastic rocks, which are part of a large igneous province (Fig. 2). This province is formed by Early-Middle Jurassic volcanism of the Lonco Trapial, Marifil and Chon Aike Formations and is also well-represented in the San Jorge Basin (Bahía Laura Group; Pankhurst et al., 1998). Coeval with this volcanic episode, the I-type, subduction-related Subcordilleran batholith was developed in the western sector of the Patagonian foreland, (Fig., 2; Rapela et al., 2005). To the east, Late Jurassic to Cretaceous sedimentary rocks of CAB comprise a thick continental sequence with high volcaniclastic input, accommodated in depocenters separated by basement uplifted blocks (Figari et al., 2015). To the south, the E-W-trending rift-related San Jorge Basin comprises Neocomian to Paleogene continental/marine deposits (Fig. 2, Sylwan et al., 2001). Farther south, sedimentary sequences of Cretaceous age are exposed in the San Bernardo fold and thrust belt being represented mainly by the Chubut Group continental deposits (Fig. 2, Homovc et al., 1995). Eastward shifts of the magmatic arc in

Paleocene-Eocene times produced ignimbritic successions that cover large areas of the broken foreland system (Folguera and Ramos, 2011; Aragón et al., 2011). Within-plate basaltic plateaus are widespread in Early Neogene times, represented by the Somuncura and Meseta Cuadrada plateaus, which are deposited in the north and south parts of the broken foreland, respectively. Finally, the Miocene-Present configuration of the Patagonian foreland is characterized by several intermontane basins with Neogene-Quaternary clastic and volcanic deposits bounded by uplifted basement blocks (Bilmes et al., 2013).

3. Integrated geophysical and structural analysis of the Patagonian foreland

3.1 Aeromagnetic and global gravity data

The aeromagnetic dataset used in this work was surveyed by the Argentinian Geological Survey (SEGEMAR) and, in the case of one block, by the Comisión Nacional de Energía Atómica (CNEA) in 1978, 1995-1996 and 1999. Four data-blocks, namely Chubut Central (surveyed by CNEA), Pilcaniyeu, Jacobacci and Esquel, (SEGEMAR, 1999a, b, and c, respectively, see Figure S1 of supplementary material for further details) were compiled and reprocessed. The "Chubut Central" aeromagnetic data was previously digitized (SEGEMAR, 2001; Álvarez, 2017). The aeromagnetic flight line spacing was of ~1000 m with most of the lines trending N-S, except in the Chubut Central block (the biggest block) where lines trend E-W. Flight height ranges from 120 to 140 m. During reprocessing, magnetic noise was detected along E-W flight lines. To eliminate it, a noise grid was subtracted from the original one. The noise grid was obtained applying a directional cosine filter in order to enhance the noise signal, with a cosine function degree of 0.5. Then, a Fast Fourier Transform and a Butterworth Filter were applied (Álvarez, 2017).

In order to check the quality of the reprocessed aeromagnetic data, a field magnetic profile was surveyed in the central part of the studied area. This profile is ~50 km long and was carried out 50 km to the north of Paso de Indios (Figs. S1 and S2 of the supplementary material), along a local road oriented ~NE-SW. A G856 Geometrics proton precession magnetometer with a resolution of 0.1 nT was used. The spacing between stations was of 500 m. Three or more observations were taken at each station and the corresponding values were averaged. Accurate position of each station was determined by GPS. Magnetic measurements were corrected for the diurnal variations in the Earth's magnetic field by data of the Trelew Geomagnetic Observatory (INTERMAGNET). The obtained ground total magnetic field was upward continued to 140 m (mean flight height) with the aim of allowing an appropriate comparison with the profile extracted from the aeromagnetic data. Both data sets (aeromagnetic and ground total magnetic field) show a good coincidence after correcting for the different acquisition dates (Fig. S2), indicating that the re-processed aeromagnetic data are reliable and appropriate for regional analysis.

For interpretation purposes, total aeromagnetic field was reduced to the pole and then upward continued to 3000 meters using Geosoft Oasis Montaj software (Fig. 3a). This processing was used to reduce the short wavelength magnetic and high amplitude signal generated by high magnetic susceptibility of the Mesozoic and Cenozoic volcanic rocks (see Fig. 2 for geographic distribution of these lithologies and Table S1 for magnetic susceptibity values) and to highlight long wavelength magnetic responses from deeper crustal sources. Tilt derivative was calculated from Reduced to Pole and Upward Continued to 2000 m data for detecting edges and extent of basement sources (Fig. 3b).

Complete Bouguer anomalies were calculated from the Eigen-6C4 global model (Förste et al., 2014) and from IGN (Instituto Geográfico Nacional) ground data. IGN ground gravity data were surveyed only along main roads as can be observed in Fig. S3 (supplementary material) consequently, IGN data coverage is partial and not suitable for our purposes. The comparison between Eigen-6C4 and IGN complete Bouguer anomalies shows large differences in the areas where there are no ground IGN data. Therefore, the Eigen-6C4 complete Bouguer anomaly is considered as the more reliable and appropriate for our regional analysis.

In order to investigate the upper crustal density distribution in Central Patagonia, the residual Bouguer anomaly was calculated subtracting the complete Bouguer anomaly upward continued to 10 km from the complete Bouguer anomaly. This reflects lateral density variations within the upper crust and permits the analysis of high-density basement blocks distribution.

3.2 Aeromagnetic data

3.2.1 Magnetic lineaments and domains

For the structural analysis of the aeromagnetic dataset, we consider that regional lineaments and fault zones separate different magnetic domains which can be characterized by magnetic intensity and texture. The analysis of gradient variation of the magnetic field (i.e. Fig. 3b) is used for detection of sources and for limiting magnetic-discrete domains (Miller and Singh, 1994; Aitken and Betts, 2009). These domains show a magnetic signature specific to the lithologies cropping out in these areas.

The aeromagnetic data shows the presence of two types of regional scale structures defined by their magnetic trend and located in different areas. In the western area and completely controlled by the structures of the Andean orogenic process, the magnetic structural trend is characterized by N-S to NNE-SSW-trending magnetic lineaments that correspond to Andean thrusts (Fig. 3c). These structures, which are related to the Andean fold and thrust belt, are exposed in the North Patagonian Andes along westernmost margin of North Patagonian Massif (Giacosa et al., 2004). To the east, the N-S to NNE-SSW magnetic structural trend is also observed in the Pampa de Agnia Thrust (Fig. 3c, PAT), a structure previously identified in regional structural cross-sections (Figari et al., 2015; Echaurren et al., 2016). The ~N-S regional magnetic lineaments developed from North Patagonian Andes to the Pampia de Agnia basin are interrupted by a general northwest trending magnetic structural anisotropy, where southwest verging thrusts are developed (Fig. 2 and 3c). Three main thrusts of previous structural studies are redefined based on the aeromagnetic interpretation: the San Bernardo Thrust (SBT) located in the San Bernardo FTB (Barcat et al., 1986; Gianni et al., 2017); the Río Chubut Medio-Taquetrén Thrust Fault (RCMF-TTF), which is the most conspicuous structure in the region (Coira et al., 1975; Bilmes et al., 2013; Figari et al., 2015; Echaurren et al., 2016); and the Gastre-Sacanana Fault (GSF), located in the northern limit of Gastre Basin (Fig 3c) and previously described by Coira et al. (1975), Rapela and Pankhurst (1992), Bilmes et al. (2013).

The Los Altares domain is characterized by high frequency and high amplitude northeast-trending magnetic trend (Fig. 3d). This domain is truncated towards the southwest by the Río Chubut Medio – Taquetrén Thrust Fault (RCMF-TTF), marking a sharp change in magnetic character which defines the eastern limit of San Bernardo domain (Fig. 3d). San Bernardo domain is characterized, in its eastern part, by a northwest elongated, low frequency magnetic minimum of

~50 km width (Fig. 3c). The southwestern portion of this domain is characterized by a northwest-elongated, low frequency magnetic maximum which shows a similar amplitude in comparison with the northeast minimum (Fig. 3c). Immediately to the northwest of San Bernardo domain, the Pampa de Agnia domain (Fig 3d) is defined by a moderate magnetic intensity signal cross-cut by alternating northeast-elongated magnetic maximums and minimums of approximately 5 km wavelength (Fig. 3c). The northern limit of Pampa de Agnia domain is defined by the (Piedra Parada Fault) PPF separating this domain from the Piedra Parada domain (Fig. 3d). Piedra Parada domain is characterized by a moderate magnetic intensity signal interrupted by alternating NE-SW elongated magnetic maximums and minimums, while in its northwestern sector a well-defined, low wavelength, magnetic maximum is detected (Fig. 3c). Pampa de Agnia domain is limited to the west by the North Patagonian Andes Thrust (NPAT, Fig. 3c). The North Patagonian Andes domain (Fig. 3d) is characterized by two distinct magnetic signatures. North of 43°S an area of homogeneous high frequency maximums and south of 43°S an area of alternating magnetic minimums and maximums of ~10 km wavelength (Fig. 3c).

Farther north, Ñirihuau domain (Fig. 3d) is characterized by moderate magnetic values and to the east limits with the Gastre domain, separated by the Chico river. The Gastre domain (Fig. 3d) is characterized by a northwest-southeast-elongated shape, with a moderate-to-low magnetic signal crosscut by magnetic maximums and minimums (Fig. 3c). The northern limit of this domain is defined by Gastre Sacanana Fault (GSF). To the southeast of Gastre domain, Taquetren and Pichiñanes domains are defined by high wavelength (between 20-10 km) magnetic minimums (Fig. 3c).

3.2.2 Interpretation

Lithologies cropping-out in Los Altares domain (Fig. 3d) are mainly Jurassic volcanic rocks (Lonco Trapial and Marifil Fm.), which are part of the siliceous Chon Aike Magmatic Province (Kay et al., 1989), showing high frequency magnetic maximums. To the west, in San Bernardo domain (Fig. 3d), two different magnetic-signature areas have been defined. The main difference between them is the absence of deformation in the easternmost area, which is characterized by a magnetic minimum. However, the westernmost area shows a NW-trending magnetic maximum (Fig. 3c) and exposes the Cretaceous Chubut Group in SBFTB (Fig. 2). The magnetic response in SBFTB could represent the subsurface presence of Jurassic volcanics (Bahia Laura Group/ Lonco Trapial Fm.) which are affected by SBT, as noted in seismic studies (Barcat et al, 1984; Gianni et al., 2015).

The Pampa de Agnia domain (Fig. 3d) is located to the northwest of San Bernardo domain and exhibits Late Paleozoic marine and continental successions covered by Liassic marine sediments. These units are intruded by Jurassic-Cretaceous plutonic and sub-volcanic rocks and covered by Cenozoic volcanics (see Fig. 2). Magnetic maximums of limited extension (Fig. 3c) are related to the latter volcanics. In Piedra Parada domain (Fig. 3d), Cenozoic volcanics are widely present (see Fig. 2). Cretaceous-Paleogene marine successions are covered by Oligocene-Early Miocene within-plate basalts and show a good correspondence with NE-SW elongated magnetic maximums (Fig. 3c). In its northwestern area, the long-wavelength magnetic maximum shows good correspondence with volcanic rocks of the Eocene Pilcaniyeu belt (Aragón et al., 2011; Ianelli et al., 2017).

To the west, in North Patagonian Andes domain (Fig. 3d), two areas have been defined. North of 43°S, the magnetic signature overlaps with the development of El Maiten fold and thrust

belt and the outcrops of the Subcordilleran batholith (Lower Jurassic plutonic rocks). South of 43°S, the magnetic signature exhibits good correspondence with Lower Cretaceous (Divisadero Group) and Jurassic volcanic rocks (Lonco Trapial Fm.) (Fig. 2). The moderate-to-low magnetic signature in Ñirihuau Domain (Fig. 3d) matches with the development of Ñirihuau-Ñorquinco volcano-sedimentary Miocene synorogenic deposits (Giacosa et al., 2005; Bechis et al., 2014; Ramos et al., 2015).

To the east, the Gastre domain (Fig. 3d) is characterized by a magnetic minimum showing good correspondence with the outcrops of Paleozoic Mamil Choique granitoids (281 ± 2 and 295 ± 2 Ma, Pankhurst et al., 2006; Varela et al., 2005), located near Río Chico. In its southeastern sector, the magnetic maximums show good coincidence with the outcrops of Lonco Trapial Formation (Jurassic volcanic rocks), which are located in the northern part of the Taquetrén Range. The Taquetrén and Pichiñanes domains (Fig. 3d) are defined by magnetic minimums which are in good correspondence with the magnetic signature of Paleozoic basement crustal blocks (Fig 4), where the Paso del Sapo granodiorite (314 ± 2 Ma, Pankhurst et al., 2006) and the Pichiñanes granite (318 ± 2 Ma, Pankhurst et al., 2006) crop out (see Fig. 1). The location of Paleozoic basement outcrops is of crucial interest for this work and will be analyzed in the following sections.

3.3 Gravimetric interpretation and its relation with basement blocks

The residual complete Bouguer anomaly correlates well with the interpreted magnetic domains and structural elements (Fig. 4a). In the residual complete Bouguer anomaly, a series of long wavelength, positive anomalies (maximum amplitude of 12.6

mGal) are aligned along the northwest-southeast trending RCMF-TTF (Río Chubut Medio Fault-Taquetrén Thrust Front) (Fig. 4a). These positive gravity anomalies coincide with the outcrops of Middle to Late Paleozoic igneous and metamorphic rocks (Fig. 4b), such as the Paso del Sapo granodiorite/granite, Pichiñanes granite and metamorphic rocks of the Cushamen Formation.

From south to north, the "Pampa de los Guanacos" positive anomaly correlates with subsurface basement drilling cores, located in the north portion of San Jorge basin, which yielded Middle Carboniferous and Early Permian K-Ar ages (Fig 4a, b, Linares and González, 1990). This block extends to the west of the RCMF-TTF, but shows maximum positive anomalies immediately to the east of this structure, suggesting the reverse faulting of the Late Paleozoic basement (Fig. 4a). To the north, La Potranca positive residual anomaly coincides with the outcrops of La Potranca leucogranite (Fig. 4a, b, 289 ± 2 Ma) which is hosted by high density metamorphic complexes conformed by migmatites and orthopyroxene granulites (Pankhurst et al., 2006). Pichiñanes northeast-southwest trending positive anomaly (Fig 4a), is lower than the anomalies observed in the rest of the blocks (~5 mGal), which could be related to the limited basement outcrops in this area, constituted by garnet-bearing leucogranites of 318 ± 2 Ma age (Pankhurst et al., 2006) with unknown hosting rocks (Fig. 4b). To the northwest, Taquetrén sector is characterized by large positive residual anomalies (Fig. 4a, 12.6 mGal) and shows good correlation with the outcrops of a Late Paleozoic igneous-metamorphic complex intruded by a foliated granodiorite and mylonitic granite (Fig. 4b, 314 ± 2 Ma, Pankhurst et al, 2006). At a distance of ~70 km, aligned with RCMF-TTF, the Río Chico area presents positive anomalies of ~8.3 mGal (Fig. 4a), and coincide with the Río Chico Complex outcrops. This complex is constituted

by tonalites (Fig, 4b, 329 ± 4 Ma, Pankhurst et al., 2006), granites, gneisses and migmatites (Dalla Salda et al., 1994; Giacosa et al., 2004). Finally, near Bariloche locality, the Cañadón de la Mosca positive anomaly (Fig. 4a) corresponds to outcrops of foliated igneous rocks, mica-schists and gneisses. These granitoids have been dated as 323 ± 3 Ma (Fig. 4b, Pankhurst et al., 2006).

The good correlation between positive Bouguer residual anomaly values and the existence of igneous-metamorphic basement is due to the presence of high-density metamorphic rocks, which are common in several outcrops along this belt. The occurrence of these basement blocks is controlled by the development of regional-scale thrust zones identified in the aeromagnetic and structural data interpretation (section 3.2.1). In previous gravity studies carried out near Gastre locality, this relationship between positive gravity anomalies values and high-density basements rock was also recognized (Lince Klinger et al., 2011).

3.4 Internal Structure of Paleozoic granitoids in Central Patagonia

We made a regional geological survey taking field structural data to compare them with aeromagnetic and gravimetric data. The structural control exerted by regional faults in the geographical distribution of igneous-metamorphic basement blocks becomes clear from Figures 4a and 4b. In particular, the control exerted by the Río Chubut Medio Fault-Taquetrén Thrust Front (RCMF-TTF) in the location of Cañadón de la Mosca, Río Chico, Taquetrén and Pichiñanes basement blocks (Fig. 5). For a proper characterization of the inherited structure influence of the Paleozoic basement complexes in the successive reactivation and development of faults, the internal structure of different syn-tectonic plutonic bodies conforming these blocks is described (Fig. 5a).

In coincidence with the Cañadón de la Mosca positive residual anomaly (Fig. 5a), the Cañadón de la Mosca Diorite (323 ± 3 Ma, Pankhurst et al., 2006) crops out. It presents a well-developed magmatic foliation defined by shape preferred orientation of plagioclase and hornblende, with a mean orientation S= 299°/43°W (Fig. 5a). In addition, and in structural concordance, magmatic layering is observed, defined by the alternation of dioritic, tonalitic and subordinated gabbroic facies (Fig. 6e).

Approximately 70 km to the southeast, in coincidence with the Río Chico positive residual gravity anomaly, the El Platero tonalite (329 ± 4 Ma, Pankhurst et al., 2006) exhibits a WNW-ESE magmatic foliation defined by shape-preferred orientation of euhedral plagioclase with a mean orientation S=285°/66°NE. this orientation is subparallel to the RCMF-TTF (Fig. 5a).

The Laguna del Toro foliated hornblende-biotite granodiorite (294 ± 2 Ma, Pankhurst et al., 2006) crops out in the northern part of Taquetrén positive residual gravity anomaly (Fig. 5a). It displays shape-preferred orientation of elongated mafic enclaves (Fig. 6c). The elongation of enclaves is parallel to a poorly defined magmatic foliation with a mean value of S= 152°/55° E (Fig. 6c).

At approximately 60 km to the southeast in the Taquetrén positive residual gravity anomaly, the Paso del Sapo granodiorite and mylonitic granite crop out (Fig. 5a). The first consists of an elongated S-type intrusion (314 ± 2 Ma, Pankhurst et al., 2006) that lie parallel to the metamorphic foliation of biotite-garnet-sillimanite gneisses and gneissic migmatites. The peraluminous Paso del Sapo granodiorite is a NW-SE elongated body, spatially associated with an almost coeval mylonitic granite (314 ± 2 Ma, Pankhurst et al.,

2006). The magmatic foliation of the Paso del Sapo granodiorite is characterized by a compositional layering of melanocratic (hbl-bt) and leucocratic (kfs-qtz) layers. A magmatic foliation defined by shape-preferred orientation of hornblende and feldspars is also observed, parallel to the magmatic layering. The mylonitic granite is found in local shear zones, parallel to the magmatic foliation of the granodiorite (S = 320°/44°E; Fig. 6a). The mylonitic foliation is defined by elongated ribbons of recrystallized quartz and feldspar and biotite-hornblende aggregates, and is parallel to the magmatic/sub-magmatic foliation of the Paso del Sapo granodiorite (Fig. 6a). A mean stretching lineation of 46°/034° is defined by elongated muscovite aggregates, whereas kinematic indicators, such as S-C structures and sigma K-Feldspars porphyroclasts, indicate reverse dip-slip and subordinated dextral strike-slip.

Further southeast, the Sierra de Pichiñanes biotite-garnet granodiorite (318 ± 2 Ma, Pankhurst et al., 2006) is exposed in coincidence with the northeast-southwest oriented Pichiñanes positive residual gravity anomaly (Fig. 5a). It shows a well-defined NW-SE magmatic foliation given by shape-preferred orientation of euhedral K-feldspar crystals with a mean foliation S= 130°/48°W (Fig. 6d).

Finally, at the southernmost basement outcrop, the La Potranca leucogranite (289 ± 2 Ma, Pankhurst et al., 2006) crops out in coincidence with the “La Potranca” positive residual gravity anomaly, intruding a migmatite and a biotite-sillimanite gneiss (Fig. 5a). Neither magmatic nor solid-state fabrics were observed in the field.

4. Discussion

4.1 Inherited structures and structural control

We have described regional-scale structures which are mappable from aeromagnetic and gravimetric data and correlate well with exposed faults. These structures control the actual setup of a series of high-density basement blocks, composed by Paleozoic igneous-metamorphic complexes and syn-tectonic granitoids (Figs. 5a, b). Igneous-metamorphic complexes and syn-tectonic granitoids provide a significant petrophysical contrast between basement blocks and Mesozoic-Cenozoic lithologies, both in gravity and in aeromagnetic results, and permit the mapping of basement crustal blocks.

For analyzing the inherited structural control in the development of Patagonian broken foreland, it is important to note that mylonitic and pre-existing basement foliations can provide a weak medium for reactivation and locus for successive fault development (White et al, 1986; Holdsworth et al., 2001). Therefore, the internal structure of Paleozoic syn-tectonic igneous bodies is considered.

We have found a general NW-SE structural trend in the internal fabric of Paleozoic granitoids (Figs. 5 and 6), which coincides with the orientation of the foliation in metamorphic host rocks (Dalla Salda, et al., 1994; Giacosa et al., 2004; Cerredo and Lopez de Lucchi, 1998; von Gosen and Loske, 2004; von Gosen, 2008; Zaffarana et al., 2010; Oriolo et al., 2019). This structural fabric found in different syntectonic plutonic bodies is defined by magmatic and solid-state processes which indicate regional deformation conditions operating during emplacement (Paterson et al., 1989). Granite emplacement is related with the development of major structures, so the location of syn-to-post-orogenic granitoids are a valuable indicator of an inherited large-scale crustal architecture (e.g. Vigneresse, 1995; Brown and Solar, 1998; Petford et al., 2000, Aitken and Betts, 2009).

In our study area, four basement localities were analyzed and the internal structure of foliated granitoids shows a close structural control in the development of the Río Chubut Medio Fault – Taquetrén Thrust Front (RCMF-TTF), which is an important regional structure previously described by various authors (Coira et al., 1975; Dalla Salda and Franseze, 1987; Bilmes et al., 2013, among others). Close to the thrust front, near the Paso del Sapo locality, the Paso del Sapo mylonitic granite shows a foliation of S=320°/44°NE, identical to RCMF, and high-angle stretching lineation (Fig. 6a). Moreover, evidence from seismic interpretation in the Taquetrén range, suggests that the Paleozoic basement fabric was reactivated as the RCMF-TTF (Echaurren et al., 2016). A similar internal structure is found in the El Platero tonalite, Laguna del Toro and Paso del Sapo granodiorites, and Sierra de Pichiñanes granite, showing magmatic structures (Fig. 5a and 6). All of these granitoids are located along the actual development of RCMF-TTF. The relationship of this inherited structural fabric with the development of a major thrust zone becomes clear when we consider that well-developed foliations in mylonites and foliated granitoids could be planes of weakness, where subsequent reactivation occurs (Watterson, 1975; White et al., 1986; Ferreira et al., 2008; Phillips et al., 2016). We consider that magmatic and mylonitic foliations developed in Late Paleozoic granitoids could represent planes of mechanical weaknesses available for successive reactivations.

The Gastre-Sacanana Fault (GSF) is located almost parallel to the Río Chubut Medio Fault – Taquetrén Thrust Front (RCMF-TTF, Figs. 4 and 5) and exposes Permian-Triassic granitoids and Paleozoic granitoids. Based on structural field data, a Late Paleozoic ~NW-SE internal structure is recognized in these granitoids (von Gosen and Loske, 2004; Zaffarana et al., 2010; 2017). We thus suggest a similar origin for both GSF and RCMF-TTF, with an internal fabric of Late Paleozoic

granitoids and associated metamorphic wall rocks generating a structural control in subsequent faulting. This area was the key locality for the proposal of the Triassic-Jurassic crustal-scale intracontinental Gastre Fault system (Rapela and Pankhurst et al., 1992), which was used in numerous Mesozoic paleogeographic reconstructions for South America (e.g. Dalziel, 1997). However, several works have put in doubt the existence of this Mesozoic shear zone (von Gosen and Loske, 2004; Zaffarana et al., 2014; Ramos et al., 2017). Based on our data, this structure can be interpreted as the result of an early reactivation of the Late Paleozoic structural fabric and, therefore, the Gastre Fault system might not have such a regional importance as previously suggested. Zaffarana et al. (2017) have indicated an emplacement history for the Triassic Central Patagonian Batholith controlled by the Late Paleozoic inherited structural fabric.

Crustal heterogeneities and long-term fault zones may represent a major factor of weakening in the continental crust (White et al., 1986; Clendenin and Diehl, 1999; Butler et al., 2006; Şengör et al., 2018). Paleozoic basement inherited structures described in this work might thus be successively reactivated, mostly as fault zones, when they were favorably oriented to the prevailing stress field and if thermo-mechanical conditions were reached (White et al., 1986; Holdsworth, 2004). According to this, the existence of a weak lithosphere has been proposed in Central Patagonia to explain the focus of intraplate deformation during different tectonic events (Bilmes et al., 2013; Echaurren et al., 2016; Gianni et al., 2015) and this zone was related with the location of basement contractional structures and intraplate rift basins (Gianni et al., 2017). Once formed, weak lithospheric fault zones remain susceptible to reactivation into transpressional or transtensional structural assemblages and can channel ore-generating fluids (Marshak and Paulsen,

1996). This is an important aspect considering that GSF control the development of the Navidad epithermal Ag-Pb world-class deposit (Bouhier et al., 2018).

4.2 Paleozoic scenario in northwestern Patagonia

Several works have indicated the presence of an active continental margin along the western North Patagonian Massif, associated with a major deformation belt (Pankhurst et al., 2006; Ramos, 2008; Varela et al., 2015; Prezzi et al., 2018; Vizán et al., 2017). The ~NW-SE magmatic and solid-state structures found in syntectonic Paleozoic granitoids coincide with the ~NE-SW tectonic shortening proposed for Late Paleozoic times in different sectors of this deformation belt (Cerredo and Lopez de Luchi, 1998; Giacosa et al., 2004; von Gosen, 2008; Oriolo et al., 2019). In addition, Renda (pers.comm.) proposes deformation in the Taquetrén range during the Devonian-Carboniferous boundary (ca. 350 Ma) that could possibly correspond to an orogenic process, whereas Oriolo et al. (2019) indicate transpressional deformation and metamorphism in the North Patagonian Andes at ca. 300 Ma, attributed to an active continental margin. The NW-SE-striking domain recognized by geophysical and field data in this work would thus represent this major Late Paleozoic orogenic belt, comprising continental arc magmatism together with associated deformation and metamorphism of basement complexes. According to Vizán et al. (2017), the deformation also included wrench tectonics due to a toroidal motion of Western Gondwana respect to Eastern Gondwana, accreting Southern Patagonia to South American plate and closing the Paleozoic magmatic arc (Varela et al., 2005; 2015). The different deformation processes developed in this margin range during this time span might favor the development of ductile structures that were later reactivated until the Late Cenozoic.

The Figure 7 shows an absolute paleomagnetic paleoreconstruction (latitudinal and longitudinal) of Gondwana for the Late Carboniferous (ca. 320 Ma). The major continents are reconstructed according to Vizán et al. (2017). Vizán et al. (2015, 2017) based their reconstruction of southern Patagonia fundamentally on the basis of paleomagnetic data obtained in strata of the Tepuel Genoa Basin of Rapalini et al. (1994). Different authors were considered to adjust the paleogeographic location of the Malvinas/Falkland Islands, the Ellsworth - Whitmore mountains of Antarctica, the block of the Thurston Island, Marie Bird Land and New Zealand (see caption in Fig. 7).

Regarding Patagonia, it is noteworthy that Ramos and Naipauer (2014), among others, have suggested that it was integrally forming a marginal land of Antarctica during the Paleozoic. For González et al. (2018), several lines of geological evidence point to a parautochthonous origin of the eastern North Patagonian Massif as an outboard assemblage that represents the conjugate margin of the Pensacola-Queen Maud-Ellsworth-Whitmore Mountains of Antarctica. The Antarctic Peninsula would have been located in the west of Southern Patagonia since the Late Paleozoic (Castillo et al., 2017). In the Malvinas/Falkland Islands and the Ellsworth Whitmore Mountains (EWM), there are also outcrops of Late Paleozoic rocks forming Du Toit´s Samfrau Geosyncline together with the Cape Fold Belt (South Africa) and the Sierras Australes of Buenos Aires (Argentina) (Curtis and Hyam, 1998). The Tepuel-Genoa basin (Fig. 7) would also be part of southern Patagonia. The Tepuel-Genoa basin, classified as a back-arc basin (Limarino and Spalletti, 2006), has very little contribution of volcanic and plutonic detritus, implying that the basin was not close to a magmatic arc during deposition (Ciccioli et al., 2018). The Middle Carboniferous-Early Permian fossil assemblage of this basin have affinities with Australian fauna of the same age and is peri-Antarctic with an approximate paleolatitude of 70 °S (Taboada and Shi,

2011). Southern Patagonia is located as a peri- Antarctic block and the southern limit of the NPM would be the southwestern margin of Gondwana. Thus, we suggest that it would correspond to an active tectonic margin from the Early Ordovician till the Early Permian.

4.3 Controls of Paleozoic structures on the Mesozoic-Cenozoic evolution of the Patagonian Foreland

During Late Triassic-Jurassic times, Patagonia underwent an extensional tectonic setting related with widespread volcanic rocks deposited in NNW-SSE-trending grabens (Fig. 8a; Uliana and Biddle, 1987; Figari et al., 2005; 2015). We consider that the Río Chubut Medio Fault – Taquetrén Thrust Front (RCMF-TTF) exerts an important structural control on the development of the main depocenters of the Cañadon Asfalto Basin (Fig. 8a), as these rift-related depocenters are generated in the hanging wall of the RCMF-TTF. The role of NW-SE Paleozoic inherited structural fabric in the Jurassic-Cretaceous depocenters was also suggested by Figari et al. (2015), but its relation with RCMF-TTF was not fully indicated. In Paso del Sapo mylonitic granite, Paleozoic reverse dextral kinematic indicators were found (section 3.4). For Late Triassic-Jurassic times, this structure can be characterized as a replacement structure, since its reactivation is in a different sense from the original one (Şengör et al., 2018), being a contractional zone reactivated as a series of minor normal faults controlling the development of depocenters.

Towards the end of the development of the Cañadon Asfalto Basin, during Late Cretaceous times, a vast marine transgression was registered in the Patagonian foreland (Fig. 8b). This event coincides with a period of high convergence registered in the Andean margin, where the highest

westward velocities of South America were achieved (Somoza and Zaffarana, 2008). Fission track data in several Paleozoic basement blocks revealed a ~124-70 Ma exhumation episode in the North Patagonian foreland (Fig. 8b; Savignano et al., 2016). In this period, the RCMF and associated synthetic faults located to the southwest and northeast acted as resurrected structures (sensu Şengör et al., 2018). In particular, the RCMF played an important role controlling the sedimentary architecture of depocenters such as the "Paso del Sapo Embayment" (Fig. 8b), a narrow, coarse-grained, tide-dominated delta deposited in a tectonically active area (Scasso et al., 2012). Moreover, the tectonic activity of Río Chubut Medio Fault- Taquetrén Thrust Front (RCMF-TTF) in Late Cretaceous times is also constrained by fans of westwards growing strata and progressive unconformities found in the ~83 Ma Paso del Sapo Formation, implying a Campanian thrusting along the RCMF-TTF (Fig. 8b, Echaurren et al., 2016).

During Paleocene-Eocene times, tectonic reconstructions show that the convergence along the South American margin was of high obliquity (Somoza and Ghidella, 2012). In this period, the activity of RCMF-TTF continues as it is defined by the exhumation of fault-controlled Paleozoic basement blocks at ~47 Ma (Fig. 8c). In the Patagonian foreland, an extensional/transtentional period initiates and widespread retro-arc, bimodal magmatism is represented by the Pilcaniyeu Belt, that spans from 60 to 42 Ma (Fig. 8c, Aragón et al., 2011; Ianelli et al., 2017). This magmatism is associated with an extensional retroarc setting (Aragón et al., 2011) and the outcrops are concentrated in Piedra Parada Domain limited by RCMF-TTF and PPF (section 3.2.2, Fig. 8c). Remarkably, this area concentrates WSW-ENE strike-slip structures probably associated with a transpressive tectonic regime (Ruiz, 2005; Figari et al., 2015). Following this line of

evidence, it should not be ruled out that RCMF-TTF and PPF could have acted as nearly parallel "en échelon" faults generating a pull apart tectonic control in magmatism.

One of the last contractional reactivation periods, which controls the actual morphology of the Patagonian broken foreland, occurs during Miocene times. Several independent intermontane basins were developed in the Andean foreland separated by basement blocks and the inversion of Mesozoic depocenters (Fig. 8d). Syntectonic sedimentation is found all along the broken foreland (Bilmes et al., 2013; Ramos et al., 2015; Echaurren et al., 2016; Gianni et al., 2017; Bucher, et al., 2019a, b) (Fig. 8d). Near the Andean domain, the main depocenter (i.e. Ñirihuau-Ñorquinco, Fig. 8d) of the Pilcaniyeu Basin is limited by two regional NW-SE thrusts (Ramos et al., 2015), which we identify as RCMF-TTF (southern limit) and GSF (northern limit). Farther east, the Miocene activity of GSF was recognized in Gastre Basin by the tilting of deposits of the Late lower Miocene La Pava Formation and the thrusting of the Pre-Jurassic basement over the Middle Jurassic deposits of the Lonco Trapial Formation (Bilmes et al., 2013). Moreover, the Miocene activity of RCMF-TTF was described recently in Paso del Sapo basin (PS, Fig. 8d), where syntectonic sedimentary sequences record a deformation along the RCMF-TTF (Bucher et al., 2019a).

5. Conclusions

In Central Patagonia, a contractional Late Paleozoic tectonic regime associated with an active Gondwana margin generated a ~NW-SE structural fabric in metamorphic and igneous rocks, which was recurrently reactivated since Mesozoic times. This inherited fabric is related to a magmatic arc, with a ~NW-SE internal structure, that formed in close relation with metamorphic complexes representing a Late Paleozoic orogenic belt. Our results suggest that the present distribution of Paleozoic basement blocks is controlled by deep-seated structures. These major crustal-scale structures are reactivated and exert an important control since Early Mesozoic times in different extensional or contractional tectonic events. In Early Jurassic – Cretaceous times, the Cañadon Asfalto Basin presents a series of ~NW-SE oriented depocenters located in the hanging wall of Río Chubut Medio Fault, which is a NW-SE structure located in previous Paleozoic syn-tectonic granitoids and mylonites. These depocenters and inherited structures are inverted in Cretaceous to Cenozoic times controlling the development of the Patagonian broken foreland. As with many long-standing deformational zones worldwide, it would be important to study with more detail and applying different methodologies the nature and importance of the deep structure of this zone.

Declaration of interests

The authors declare that they have no known competing financial interests or personal relationships that could have appeared to influence the work reported in this paper.

The authors declare the following financial interests/personal relationships which may be considered as potential competing interests:

Acknowledgement

It is specially appreciated the collaboration of the "Servicio Geológico Minero Argentino" (SEGEMAR) in the use of the magnetic database. Special thanks for financial support of Agencia Nacional de Promoción Científica y Tecnológica (PICT2017 -0709), Universidad de Buenos Aires (UBACyT 20020150100069BA) and the National Geographic Society (grant CP-123R-17). Emiliano Renda thanks Dr. Andrés Echaurren for meaningful discussions. Proffesor Victor Ramos and Professor Peter Betts are acknowledged for their helpful comments to improve this manuscript. All data used in the manuscript are available in the text, figures and Supporting Information (Figures S1, S2 and S3, Tables S1 and S2). In the case of previously published data, they are referred to their source, which are listed in the References.

References

Aitken A. R. A., Betts, P. G., 2009. Multi-scale integrated structural and aeromagnetic analysis to guide tectonic models: An example from the eastern Musgrave Province, Central Australia. Tectonophysics. Vol. 476, Issues 3-4, pp: 418-435.

Alvarez, D., 2017. Reprocesamiento de los datos de magnetometría aérea del Bloque 13 – Chubut Central. Instituto de Geología y Recursos Minerales, SEGEMAR, Serie Contribuciones Técnicas Geofísica 15: 8 pp, Buenos Aires.

Anselmi, G., Panza, J.L., Cortés, J.M.D., Ragona, D. y Genini, A., 2004. Hoja Geológica 4569-II, El Sombrero, Provincia de Chubut. Instituto de Geología y Recursos Minerales, Servicio Geológico Minero Argentino, Boletín 271: 70 pp., Buenos Aires.

Aragón, E., D' Eramo, F., Castro, A., Pinotti, L., Brunelli, D., Rabbia, O., Rivalenti, G.,Varela, R., Spakman, W., Demartis, M., Cavarozzi, C., Aguilera, Y., Mazzucchelli, M., Ribot, A., 2011. Tectono-magmatic response to major convergence changes in the North Patagonian suprasubduction system; the Paleogene subduction–transcurrent plate margin transition. Tectonophysics 509, 218–237.

Ardolino, A., Lizuaín, A. y Salani, F. 2001. Carta Geológica Gan Gan 4369-II. SEGEMAR, B 317.Buenos Aires. Ardolino, A., Lizuaín, A. y Salani, F. 2001. Carta Geológica Gan Gan 4369-II. SEGEMAR, B 317.Buenos Aires.

Barcat, C., Cortiñas, J.S., Nevistic, V.A., Stach, N.H. y Zucchi, H.E. 1984. Geología de la región comprendida entre los lagos Musters - Colhue Huapi y la Sierra Cuadrada,

departamento Sarmiento y Paso de indios, provincia de Chubut. 9° Congreso Geológico Argentino (Bariloche), Actas 2: 263-282. Buenos Aires.

Bechis, F., Encinas, A., Concheyro, A., Litvak, V.D., Aguirre-Urreta, B., Ramos, V., 2014. New age constraints for the Cenozoic marine transgressions of northwestern Patagonia, Argentina (41°-43° S): Paleogeographic and tectonic implications. Journal of South American Earth Sciences 52, pp 72-93. https://doi.org/10.1016/j.jsames.2014.02.003

Bilmes, A., D´Elia, L., Franzese, J.R., Veiga, G.D., Hernández, M., 2013. Miocene block uplift and basin formation in the Patagonian foreland: The Gastre Basin, Argentina. Tectonophysics 601, 98 111. https://doi.org/10.1016/j.tecto.2013.05.001.

Bouhier, V.,Marta, F. , Tornos, F., Rainoldi, A., Patrier, P., Beaufort, D., 2018. Genesis of the Loma Galena deposit, Navidad district, Patagonia, Argentina. 15th Quadrennial IAGOD International Association on the Genesis of Ore Deposits Symposium, Salta, Argentina, A23, pp. 52-53.

Bracaccini, O. I., 1960. Lineamiento principales de la evolución estructural de la Argentina. Inst. Arg. Petrol., Petrotecnia X (6): 57-69, Bs. As.

Brown M., Solar, G.S., 1998. Shear-zone systems and melts: feedback relations and self-organization in orogenic belts. Journal of Structural Geology, Vol. 20, No. 213, pp. 211-227.

Bucher, J., García, M., López, M., Milanese, F., Bilmes, A., D'Elia, L., Naipauer, M., Sato, A.M., Funes, D., Rapalini, A., Franzese, J., 2019a. Tectonostratigraphic evolution and timing deformation in the Miocene Paso del Sapo Basin: implications for the Patagonian Broken Foreland. J. S. Am. Earth Sci. 94, 102212.

Bucher, J., Milanese, F., López, M., García, M., D'Elia, L., Bilmes, A., Naipuer, M., Sato, A., Funes, D., Rapalini, A., Valencia, V., Ventura Santos, R., Hauser, N., Cruz Vera, L., Franzese, J. 2019b. U-PB geochronology and magnetostratigraphy of a North Patagonian syn-orogenic Miocene succession: tectono-stratigraphic implications for the foreland system configuration. Tectonophysics. 766: 81-93. https://doi.org/10.1016/j.tecto.2019.05.021

Butler, R.; Tavarnelli, E.; Grasso, M. 2006. Structural inheritance in mountain belts: An Alpine-Apennine perspective. Journal of Structural geology 28: 1893-1908.

Castillo, P., Fanning, C.M., Pankhurst, R.J., Hervé, F., Rapela, C., 2017. Zircon O- and Hf-isotope constraints on the genesis and tectonic significance of Permian magmatism in Patagonia. J. Geol. Soc. London. 174, 803–816. https://doi.org/10.1144/jgs2016-152

Cerredo, M.E., López De Luchi, M.G., 1998. Mamil choique granitoids, southwestern North Patagonian Massif, Argentina: Magmatism and metamorphism associated with a polyphasic evolution. J. South Am. Earth Sci. 11, 499–515. https://doi.org/10.1016/S0895-9811(98)00025-X

Ciccioli, P. & Limarino, C., & Taboada, A., & Isbell, J. & Gulbranson, E. 2018. Composición modal y procedencia del Grupo Tepuel, provincia de Chubut, Argentina. VII SAPS - VII Simposio Argentino del Paleozoico Superior. Revista Del Museo de la Plata. Vol. 3, Núm. 1, La Plata, Buenos Aires, Argentina.

Clendenin, C.W., Diehl, S.F., 1999. Structural styles of Paleozoic intracratonic fault reactivation: a case study of the Grays Point fault zone in southeastern Missouri, USA. Tectonophysics, 305. 235-248.

Coira, B.L., Nullo, F.E., Proserpio, C., Ramos, V.A., 1975. Tectónica de basamento de la región occidental del Macizo Nordpatagónico, provincias de Río Negro y Chubut. Revista de la Asociación Geológica Argentina. 30(4), 361- 383.

Curtis, M. L. & Hyam, D. M. 1998. Late Palaeozoic to Mesozoic structural evolution of the Falkland Islands: a displaced segment of the Cape Fold Belt. Journal of the Geological Society, London, 155, 115-129.

Dalla Salda, L., Franzese J., 1987. Las megaestructuras del Macizo y Cordillera Norpatagónica Argentina y la génesis de las cuencas volcanosedimentarias Terciarias, Rev. Geol. Chile, 31, 3–13.

Dalla Salda, L.H.; Cingolani, C.A.; Varela, R. 1991. El basamento cristalino de la región norpatagónica de los Lagos Gutiérrez, Mascardi y Guillelmo, Provincia de Río Negro. Revista de la Asociación Geológica Argentina 46 (3-4): 263-276.

Dalla Salda, L.H., Varela, R., Cingolani, C., Aragón, E., 1994. The Rio Chico Paleozoic crystalline complex and the evolution of Northern Patagonia. J. South Am. Earth Sci. 7, 377–386. https://doi.org/10.1016/0895-9811(94)90022-1

Daly, M.C., Chorowicz, J. & Fairhead, J.D. 1989. Rift basin evolution in Africa: the influence of reactivated steep basement shear zones. *In:* Cooper, M.A. & Williams, G.D. (eds) *Inversion Tectonics*. Geological Society, London, Special Publications, **44,** 309–334.

DeCelles, P.G. 2004. Late Jurassic to Eocene evolution of the Cordilleran thrust belt and foreland basin system, western U.S.A. American Journal of Science, 304, 105–168.

Echaurren, A., Folguera, A., Gianni, G., Orts, D., Tassara, A., Encinas, A., Giménez, M., Valencia, V., 2016. Tectonic evolution of the North Patagonian Andes (41–44 S) through recognition of syntectonic strata. Tectonophysics 677-678, 99–114

Faccena, C., Nalpas, T., Brun J.P. Davy, P., Bosi, V., 1995. The influence of pre-existing thrust faults on normal fault geometry in nature and in experiments. Journal of Structural Geology. Vol. 17, No. 8, pp. 1139-1149.

Fernández Paz, L., Litvak, V.D., Echaurren, A., Iannelli, S.B., Encinas, A., Folguera, A., Valencia, V. 2018. Late Eocene volcanism in North Patagonia (42°30´-43°S): Arc resumption after a stage of within-plate magmatism. Journal of Geodynamics 113,13-31. https://doi.org/10.1016/j.jog.2017.11.005

Feruglio E., 1949. Descripción geológica de la Patagonia. Y.P.F., Bs As., 1,2 y 3.

Ferreira, J.M., Bezerra, F.H.R., Sousa, M.O.L., do Nascimento, A.F., Sá, J.M., França, G.S., 2008. The role of Precambrian mylonitic belts and present-day stress field in the coseismic reactivation of the Pernambuco lineament, Brazil. Tectonophysics 456, 111–126.

Figari, E.G., Courtade, S.F., 1993. Evolución tectosedimentaria de la cuenca de Cañadón Asfalto, Chubut, Argentina. XII Congreso Geológico Argentino y II Congreso de Exploración de Hidrocarburos, pp. 66–77

Figari, E.G., 2005. Evolución tectónica de la Cuenca de Cañadón Asfalto (Zona del valle medio del Río Chubut) Doctoral Thesis Universidad de Buenos Aires.

Figari, E.G., Scasso, R.A., Cúneo, R.N., Escapa, I., 2015. Estratigrafia y evolución geológica de la cuenca de cañadón asfalto, provincia de Chubut, Argentina. Lat. Am. J. Sedimentol. Basin Anal. 22, 11–70.

Folguera, A., Ramos, V.A., 2011. Repeated eastward shifts of arc magmatism in the Southern Andes: A revision to the long-term pattern of Andean uplift and magmatism. J. South Am. Earth Sci. 32, 531–546. https://doi.org/10.1016/j.jsames.2011.04.003

Förste, Christoph; Bruinsma, Sean.L.; Abrikosov, Oleg; Lemoine, Jean-Michel; Marty, Jean Charles; Flechtner, Frank; Balmino, G.; Barthelmes, F.; Biancale, R., 2014. EIGEN-6C4 The latest combined global gravity field model including GOCE data up to degree and order 2190 of GFZ Potsdam and GRGS Toulouse. GFZ Data Services. http://doi.org/10.5880/icgem.2015.1

Forsythe, R., 1982. The late Palaeozoic to early Mesozoic evolution of southern South America: a plate tectonic interpretation. J. Geol. Soc. London. 139, 671–682. https://doi.org/10.1144/gsjgs.139.6.0671

Fossen H., Fazli Khani H. Faleide J. I., Ksienzyk A. K. and Dunlap W. J., 2016. Post-Caledonian extension in the West Norway–northern North Sea region: the role of structural inheritance, Geological Society, London, Special Publications, 439, 465-486, 5. https://doi.org/10.1144/SP439.6

Franchi, M., Ardolino, A. y Remesal, M. 2001. Hoja Geológica Nº4166-III. Cona Niyeu. Provincia de Río Negro. Instituto de Geología y Recursos Minerales. Servicio Geológico y Minero Argentino. Boletín 262: 114p.

García-Sansegundo, J., Farias, P., Gallastegui, G., Giacosa, R.E., Heredia, N., 2009. Structure and metamorphism of the Gondwanan basement in the Bariloche region (North Patagonian Argentine Andes). Int. J. Earth Sci. 98, 1599–1608. https://doi.org/10.1007/s00531-008-0330-3

Giacosa, R., Heredia, N., César, O., Zubia, M., 2001. Hoja Geológica 4172-IV, San Carlos de Bariloche (provincias de Río Negro y Neuquén), Boletín 279. Instituto de Geología y Recursos Minerales, Servicio Geológico Minero Argentino, Buenos Aires, pp. 67.

Giacosa, R., Márquez, M., Nillni, A., Fernández, M., Fracchia, D., Parisi, C., Afonso, J., Paredes, J., Sciutto, J., 2004. Litología y estructura del basamento ígneo-metamórfico del borde SO del Macizo Nordpatagónico al oeste del río Chico, (Cushamen, Chubut, 42° 10′S - 70° 30′O). Rev. la Asoc. Geol. Argentina 59, 569–577.

Giacosa, R.E., N. Heredia, C., 2004. Structure of the North Patagonian thick-skinned fold-and-thrust belt, southern central Andes, Argentina (41°-42°S). J. South Am. Earth Sci 18, 61–72. https://doi.org/10.1016/j.jsames.2004.08.006

Giacosa, R., Afonso, J., Heredia, N., Paredes, J.M., 2005. Tertiary tectonics of the subandean region of the North Patagonian Andes, Southern central Andes of Argentina (41–42 30´ S). Journal of South American Earth Sciences 20 (3), 157– 170

Giacosa, R., Fracchia, D., Heredia, N., 2012. Structure of the Southern Patagonian Andes at 49°S, Argentina. Geol. Acta 10, 265–282. https://doi.org/10.1344/105.000001749

Giacosa, R.E., González, P.D., Nieto, D.S., Busteros, A., Lagorio, S., 2014. Metamórfismo De Alto Grado En El Basamento De Gastre, Macizo Nordpatagónico (Chubut) XIX Congreso Geológico Argentino, Córdoba, Argentina. 1, 1–2.

Gianni, G., Navarrete, C., Orts, D., Tobal, J., Folguera, A., Giménez, M., 2015. Patagonian broken foreland and related synorogenic rifting: The origin of the Chubut Group Basin. Tectonophysics 649, 81–99. https://doi.org/10.1016/j.tecto.2015.03.006

Gianni, G.M., Echaurren, A., Folguera, A., Likerman, J., Encinas, A., García, H.P.A., Dal Molin, C., Valencia, V.A., 2017. Cenozoic intraplate tectonics in Central Patagonia: Record of main Andean phases in a weak upper plate. Tectonophysics 721, 151– 166. https://doi.org/10.1016/j.tecto.2017.10.005

González, P., Coluccia, A., & Franchi, M., 1999. Geología y Recursos Minerales de la Hoja 4169-III "Ingeniero Jacobacci" (Provincia de Río Negro). Escala: 1:250.000. Servicio Geológico MineroArgentino. Subsecretaría de Minería de la Nación. Boletín N° 311. Buenos Aires.

González, P.D., Sato, A.M., Naipauer, M., Varela, R., Basei, M., Sato, K., Llambías, E.J., Chemale, F., Dorado, A.C., 2018. Patagonia-Antarctica Early Paleozoic conjugate margins: Cambrian synsedimentary silicic magmatism, U-Pb dating of Kbentonites, and related volcanogenic rocks. Gondwana Research 63, 186–225. https://doi.org/10.1016/J.GR.2018.05.015

Haller, M., Lech, R., Martínez, O., Meister, C. y Poma, S. 2010. Descripción geológica de la Hoja 4372-III y IV, Trevelin, Prov. de Chubut. Servicio Geológico Minero Argentino, Instituto de Geología y Recursos Minerales, Boletín 322, 86 p.

Hervé, F., Haller, M., Duhart, P., Fanning, M., 2005. SHRIMP U-Pb ages of detrital zircons from Cushamen and Esquel formations, North Patagonian Massif, Argentina: geological implications. 15° Congreso Geológico Argentino 1, 309-314. La Plata (Buenos Aires).

Homovc, J., Conforto, G., Lafourcade, P., Chelotti, L., 1995. Fold Belt in the San Jorge Basin, Argentina: An Example of Tectonic Inversion. In: P. Buchanan, J. y Buchanan (Eds.), Basin Inversion, Geological Society Special Publication, pp. 235–248.

Holdsworth, R.E., Hand, M., Miller, J.A. & Buick, I.S. 2001. Continental reactivation and reworking: an introduction. In: Miller, J.A., Holdsworht, R.E., Buick, I.S. & Hand, M. (eds) Continental Reactivation and Reworking. The Geological Society, London, Special Publications, 184 I-12.

Holdsworth, R. E., 2004. Weak faults—rotten cores. *Science* **303**, 181–182

Jacobs, J. & Thomas, B. 2004. A Himalayan-type indenter-escape tectonic model for the southern part of the Late Neoproterozoic Early Paleozoic East African-Antarctic Orogen. Geology. 32. 721-724. 10.1130/G20516.1.

Jordan, T., Allmendinger, R. 1986. The Sierras Pampeanas of Argentina: a modern analogue of Laramide deformation. American Journal of Science 286, 737-764.

Kay, S.M., Ramos, V. A., Mpodozis, C., Sruoga, P., 1989. Late Paleozoic to Jurassic silicic magmatism at the Gondwana margin: Analogy to the Middle Proterozoic in North America? Geology, v. 17, p 324-328.

Lacassie, J.R; Hervé, F.; Roser, B. 2006. Sedimentary provenance of the post-Early Permian to pre-Early Cretaceous metasedimentary Duque de York Com-plex, Chile. Revista Geológica Chile 33 (2): 199-219.

Lawver L, Scotese CR., 1987. A revised reconstruction of Gondwanaland. In: McKenzie GD (ed.) Gondwana six: Structure, Tectonics and Geophysics. Am Geophys Union Monogr 40:17–23

Lesta, P., Ferello, R., Chebli, G., 1980. Chubut Extraandino. In: Segundo Simposio Geología Regional Argentina, Academia Nacional de Ciencias, Córdoba 2, pp. 1306–1387.

Limarino, C.O.; Spalletti, L.A. 2006. "Paleogeography of the upper Paleozoic basins of southern South America: An overview". Journal of South American Earth Sciences. 22(3-4):134-155

Linares, E., González, R.R., 1990. Catálogo de edades radimétricas de la República Argentina 1957-1987. Asociación Geológica Argentina, Publicaciones Especiales Serie B, Didáctica y Complementaria, vol. 19, 628 pp.

Lince Klinger Federico; Martinez M. P.; Gimenez M. E.; Ruiz F.; Álvarez O. 2011. Modelo gravimétrico en la Fosa de Gastre, Provincia de Chubut, Argentina. Boletín Geológico y minero de España, 122 (3): 299-310

López de Luchi, M.G., Cerredo, M.E., 2008. Geochemistry of the Mamil Choique granitoids at Rio Chico, Río Negro, Argentina: Late Paleozoic crustal melting in the North Patagonian Massif. J. South Am. Earth Sci. 25, 526–546. https://doi.org/10.1016/j.jsames.2007.05.004

Marshak, S., Pauls, T. 1996. Midcontinent U.S. fault and fold zones: A legacy of Proterozoic intracratonic extensional tectonism? Geology, v.24; no 2: p. 151-154.

Martínez, J.C., Dristas, J.A., Massonne, H.-J., 2012. Palaeozoic accretion of the microcontinent Chilenia, North Patagonian Andes: high-pressure metamorphism and subsequent thermal relaxation. Int. Geol. Rev. 54, 472–490. https://doi.org/10.1080/00206814.2011.569411

Mundl, A., Ntaflos, T., Ackerman, L., Bizimis, M., Bjerg, E.A., Wegner, W., Hauzenberger, C.A., 2016. Geochemical and Os-Hf-Nd-Sr isotopic characterization of north patagonian mantle xenoliths: Implications for extensive melt extraction and percolation processes. J. Petrol. 57, 685–715. https://doi.org/10.1093/petrology/egv048

Navarrete, C., Gianni, G., Echaurren, A., Kingler, F. y Folguera, A. 2016. Episodic Jurassic to Lower Cretaceous intraplate compression in Central Patagonia during Gondwana breakup. Journal of Geodynamics 102C: 185-201.

Oriolo S., Schulz, B., González, P.D., Bechis, F., Olaizola, E., Krause, J., Renda, E.M., Vizán, H, 2019. The Late Paleozoic tectonometamorphic evolution of Patagonia revisited: Insights from the pressure-temperature-deformation-time (P-T-D-t) path of the Gondwanide basement of the North Patagonian Cordillera (Argentina). Tectonics 38, 2378-2400. https://doi.org/10.1029/2018TC005358

Orts, D.L., Folguera, A., Encinas, A., Ramos, M., Tobal, J.,Ramos, V.A., 2012. Tectonic development of the north Patagonian Andes and their related Miocene foreland basin (41°30´ - 43° S). Tectonics 31, 1-24.

Pankhurst, R.J., Rapela, C.W., Fanning, C.M., Márquez, M., 2006. Gondwanide continental collision and the origin of Patagonia. Earth-Science Rev. 76, 235–257. https://doi.org/10.1016/j.earscirev.2006.02.001

Paterson, S.R., Vernon, R.H., Tobisch, O.T., 1989. A review of criteria for the identification of magmatic and tectonic foliations in granitoids,Journal of Structural Geology,Volume 11, Issue 3, Pages 349-363. https://doi.org/10.1016/0191-8141(89)90074-6.

Petford, N., Cruden, A.R., McCaffrey, K.J.W., Vigneresse, J.L., 2000. Granite magma formation, transport and emplacement in the Earth's crust. Nature 408 (6813), 669–673.

Pezzuchi, H. D. 2011. Hoja Geológica Sarmiento (4569-III), Provincia del Chubut, SEGEMAR, sin texto. Carta Geológica de la República Argentina, escala 1: 250.000.

Phillips, T.B., Jackson, C.A.L., Bell, R. E., Duffy, O. B., Fossen, H., 2016. Reactivation of intrabasement structures during rifting: A case study from offshore southern Norway. *Journal of Structural Geology*. doi: 10.1098/rsta.1986.0026

Ramos, M.E., Tobal, J.E., Sagripanti, L., Folguera, A., Orts, D.L., Giménez, M., Ramos, V.A., 2015. The North Patagonian orogenic front and related foreland evolution during the Miocene, analyzed from synorogenic sedimentation and U/Pb dating (~42° S). J. S. Am. Earth Sci. 64, 467–485

Ramos, V. A., 2008. Patagonia: A paleozoic continent adrift? J. South Am. Earth Sci. 26, 235–251. https://doi.org/10.1016/j.jsames.2008.06.002

Ramos, V.A., Cingolani, C., Chemale Junior, F., Naipauer, M., Rapalini, A. 2017. The Malvinas (Falkland) islands revisited: The tectonic evolution of southern Gondwana based on U-Pb and Lu-Hf detrital zircon isotopes in the Paleozoic cover, Journal of South American Earth Sciences, doi: 10.1016/j.jsames.2016.12.013.

Randall, D.E., & Mac Niocaill, C. 2004. Cambrian Palaeomagnetic Data Confirm a Natal Embayment location for the Ellsworth-Whitmore Mountains, Antarctica, in Gondwana Reconstructions. Geophysical Journal International, 157, 105-116.

Rapalini, A., Tarling, D.,Turner, P., Flint, S. F., Vilas, J., 1994. Paleomagnetism of the Carboniferous Tepuel Group, Central Patagonia, Argentina. Tectonics. 13. 1277-1294. 10.1029/94TC00799.

Rapela, C.W., Pankhurst, R.J., 1992. The granites of northern Patagonia and the Gastre Fault System in relation to the break-up of Gondwana. In: Storey, B.C., Alabaster, T., Pankhurst, R.J. (Eds.), Magmatism and the Causes of Continental Break-Up. Geological Society of London Special Publication, vol. 68, pp. 209-220.

Rapela, C.W., Pankhurst, R.J., Fanning, C.M., Hervé, F., 2005. Pacific subduction coeval with the Karoo mantle plume: the early Jurassic Subcordilleran Belt of northwestern Patagonia. In: Vaughan, A.P.M., Leat, P.T., Pankhurst, R.J. (Eds.), Terrane Accretion Processes at the Pacific Margin of Gondwana. Geological Society of London, pp. 217–239 Special Publication 246.

Ravazzoli, I. and Sesana, F.L. 1977. Descripción geológica de la Hoja 41c, Río Chico, provincia de Río Negro. In *Servicio Geológico Nacional, Buenos Aires, Argentina*, 80 p. Boletín 148.

Remesal, M. B.; Salani, F. M.; Franchi, M. R.; Ardolino, A. A. Hoja Geológica 4169-IV Maquinchao. Boletin del Servicio Geológico Argentino. Buenos Aires. 2001 p. 1 - 68

Ruiz, L., Scasso, R. A, Aberhan, M., Kiessling, W., Bande, A., Medina, F. y S. Weidemeyer, 2005. La Formación Lefipán en el Valle medio del río Chubut: ambientes sedimentarios y su relación con la tectónica del Cretácico tardio-Paleoceno. *Actas del XV Congreso Geológico Argentino*, 3: 231-238. La Plata.

Sacomani, L.E., Panza, L., G., Parisi y H., Pezzuchi, 2007. Hoja Geológica 4366-III (Las Plumas), Provincia del Chubut, Boletín N° 291, 80 p. SEGEMAR. Buenos Aires.

Scasso, R.A., Aberhan, M., Ruiz, L., Weidemeyer, S., Medina, F.A., Kiessling, W. 2012. Integrated bio- and lithofacies analysis of coarse-grained, tide-dominated deltaic environments across the Cretaceous/Paleogene boundary in Patagonia, Argentina. Cretaceous Research 36. p. 37-57.

SEGEMAR, 1999a. Levantamiento geofísico aéreo (magnetometría y espectrometría de rayos gamma) Área Pilcaniyeu. Datos digitales. Servicio Geológico Minero Argentino.

SEGEMAR, 1999b. Levantamiento geofísico aéreo (magnetometría y espectrometría de rayos gamma) Área Jacobacci. Datos digitales. Servicio Geológico Minero Argentino.

SEGEMAR, 1999c. Levantamiento geofísico aéreo (magnetometría y espectrometría de rayos gamma) Área Esquel. Datos digitales. Servicio Geológico Minero Argentino.

SEGEMAR, 2001. Relevamiento geofísico del Bloque Chubut Central, datos magnetométricos y espectrometría de rayos gamma, digitalización y reprocesamiento de datos obtenidos por la CNEA en 1978.

Şengör, A.M.C., Lom, N., Sagdic, N.G., 2018. Tectonic inheritance, structure reactivation and lithospheric strength: the relevance of geological history. From: Wilson, R. W., Houseman, G.A., MacCaffrey, K.J.W., Doré, A.G. and Buiter, S.J.H (eds). Fifty Years of the Wilson Cycle Concept in Plate Tectonics. Geological Society, London, Special Publications, 470, https://doi.org/10.1144/SP470.8

Silva Nieto, D.G., 2005. Hoja Geológica 4369-III, Paso de Indios, provincia del Chubut. Instituto de Geología y Recursos Minerales, Servicio Geológico Minero Argentino, Boletín 265, 72 pp. Buenos Aires.

Somoza, R., Zaffarana, C.B., 2008. Mid-Cretaceous polar standstill of South America, motion of the Atlantic hotspots and the birth of the Andean cordillera. Earth Planet. Sci. Lett. 271, 267–277

Somoza, R., Ghidella, M.E., 2012. Late Cretaceous to recent plate motions in western South America revisited. Earth Planet. Sci. Lett. 331, 152–163.

Sykes, L. R., Intraplate seismicity, reactivation of preexisting zones of weakness, alkaline magmatism, and other tectonism postdating continental fragmentation, Rev. Geophys., 16, 621-688, 1978.

Sylwan, C.A., 2001. Geology of the Golfo San Jorge Basin, Argentina. Journal of Iberian Geology, 27, 123–157.

Taboada, A. C. and Shi, G. R. 2011, Taxonomic review and evolutionary trends of Levipustulini and Absenticostini (Brachiopoda) from Argentina: palaeobiogeographic and palaeoclimatic implications, Memoirs of the Association of Australasian Palaeontologists, vol. 41, pp. 87-114.

Tesauro M., Kaban M. K., Sierd A.P.L. Cloetingh, 2009. A new thermal and rheological model of the European lithosphere, Tectonophysics, Volume 476, Issues 3–4, Pages 478-495, https://doi.org/10.1016/j.tecto.2009.07.022.

Turner, J. C. M., 1965. Estratigrafía de la comarca Junín de los Andes (Neuquén). Acad. Nac. Cienc., vol. 44:5-51, Córdoba.

Uliana, M.A., Biddle, K.T., 1987. Permian to Late Cenozoic evolution of northern Patagonia: main tectonic events, magmatic activity, and depositional trends. Gondwana Six: Structure, Tectonics, and Geophysics, pp. 271–286.

Varela, R., Basei, M.A.S., Cingolani, C.A., Siga Jr., O., Passarelli, C. R., 2005. El Basamento Cristalino de los Andes norpatagónicos en Argentina: geocronología e interpretación tectónica. Revista Geológica de Chile 32, 167–182.

Varela, R., Gregori, D.A., Gonzalez, P.D., Basei, M.A.S., 2015. Caracterización geoquímica del magmatismo de arco Devónico y Carbonífero-Pérmico en el Noroeste de Patagonia, Revista de la Asociación Geológica Argentina 72, 419–432.

Vigneresse J. L., 1995. Control of granite emplacement by regional deformation. Tectonophysics 249, 173-186.

Vizán, H., Prezzi, C., Japas, M. S., Van Zele, M. A., Geuna, S. E., Renda, E. M., 2015. Tracción de losa en el margen boreal del océano paleotetis y deformación en el interior de Gondwana (incluyendo el cordón plegado de Ventana). *Revista de la Asociación Geológica Argentina*, *72*(3), 355-377.

Vizán H., Prezzi C. B., Geuna S. E., Japas M. S., Renda E. M., Franzese J., Van Zele M. A., 2017. Paleotethys slab pull, self-lubricated weak lithospheric zones, poloidal and toroidal plate motions, and Gondwana tectonics. *Geosphere*; 13 (5): 1541–1554. doi: https://doi.org/10.1130/GES01444.1

Volkheimer, W. 1964. Estratígrafía de la zona extra-andina del Departamento de Cushamen (Chubut)entre los paralelos 42° y 42°30' y los meridianos 70° X771? Asoc. Geol. Arg., Rev., XIX: 85-107. Buenos Aires

von Gosen, W. and Loske, W., 2004. Tectonic history of the Calcatapul Formation, Chubut province, Argentina, and the "Gastre fault system." J. South Am. Earth Sci. 18, 73–88. https://doi.org/10.1016/j.jsames.2004.08.007

von Gosen, W., 2008. Stages of Late Palaeozoic deformation and intrusive activity in the western part of the North Patagonian Massif (southern Argentina) and their geotectonic implications. Geol. Mag. 146, 48–71. https://doi.org/10.1017/s0016756808005311

Watterson, J. 1975. Mechanisms for the persistence of tectonic lineaments. *Nature, Lond.* 253, 520-522.

White, S.H., Bretan P.G., Rutter, E.H., 1986. Fault-Zone Reactivation: Kinematics and Mechanisms. *Phil. Trans. R. Soc. Lond. A* 317, 81-97. doi: 10.1098/rsta.1986.0026

Zaffarana, C.B., López de luchi, M.G., Somoza, R., Mercader, R., Giacosa, R., Martino, R.D. 2010. Anisotropy of magnetic susceptibility study in two classical localities of the

Gastre Fault System, central Patagonia. *Journal of South American Earth Sciences*, **30**, 151–166

Zaffarana, C.B., Somoza, R., and López de Luchi, M., 2014, The Late Triassic Central Patagonian Batholith: Magma hybridization, 40Ar/39Ar ages and thermobarometry: Journal of South American Earth Sciences, v. 55, p. 94–122, doi:10.1016/j.jsames.2014.06.006.

Zaffarana C. B., Somoza R., Orts D. L., Mercader R., Boltshauser B., Ruiz González V., Puigdomenech C., 2017. Internal structure of the Late Triassic Central Patagonian batholith at Gastre, southern Argentina: Implications for pluton emplacement and the Gastre fault system. Geosphere ; 13 (6): 1973–1992. doi:10.1130/GES01493.1

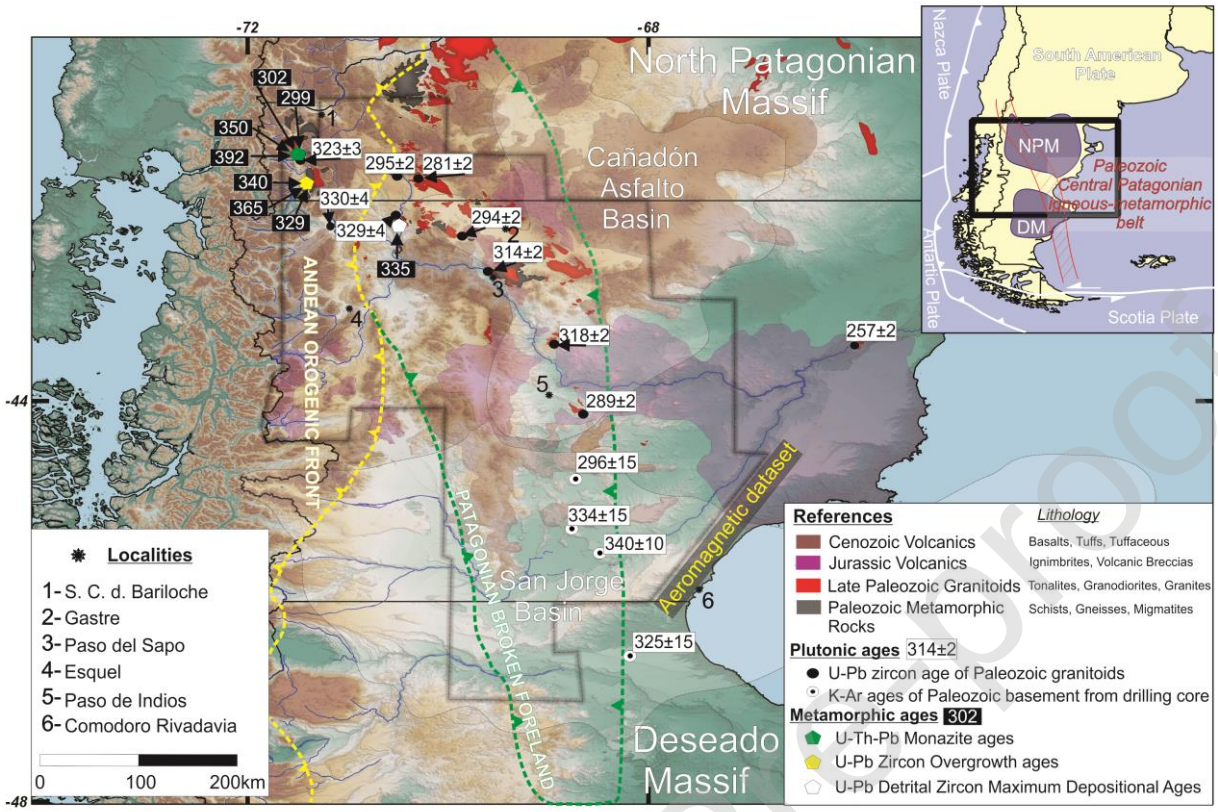

Figure 1. Geological map of the studied area. The Paleozoic basement continues in subsurface, under San Jorge Basin deposits. U-Pb zircon ages of granitoids are from Varela et al. (2005) and Pankhurst et al. (2006). K-Ar subsurface drill cores ages are from Lesta et al. (1980) and Linares and González (1990). Detrital maximum sedimentation ages are from Hervé et al. (2005) and zircon overgrowths of the El Maiten Gneiss are from Pankhurst et al (2006). Monazite Th-U-Pb ages are from Martinez et al. (2012) and Oriolo et al. (2019). Geochronological data is available at supplementary material (Table S2). Geological data modified from Giacosa et al. (2001), González et al. (1999), Remesal et al. (2001), Franchi et al. (2001), Ardolino et al. (2001), Anselmi et al. (2004), Sacomani

et al. (2007), Silva Nieto (2005), Haller et al. (2010) and Pezzuchi (2011). NPM: North Patagonian Massif, DM: Deseado Massif.

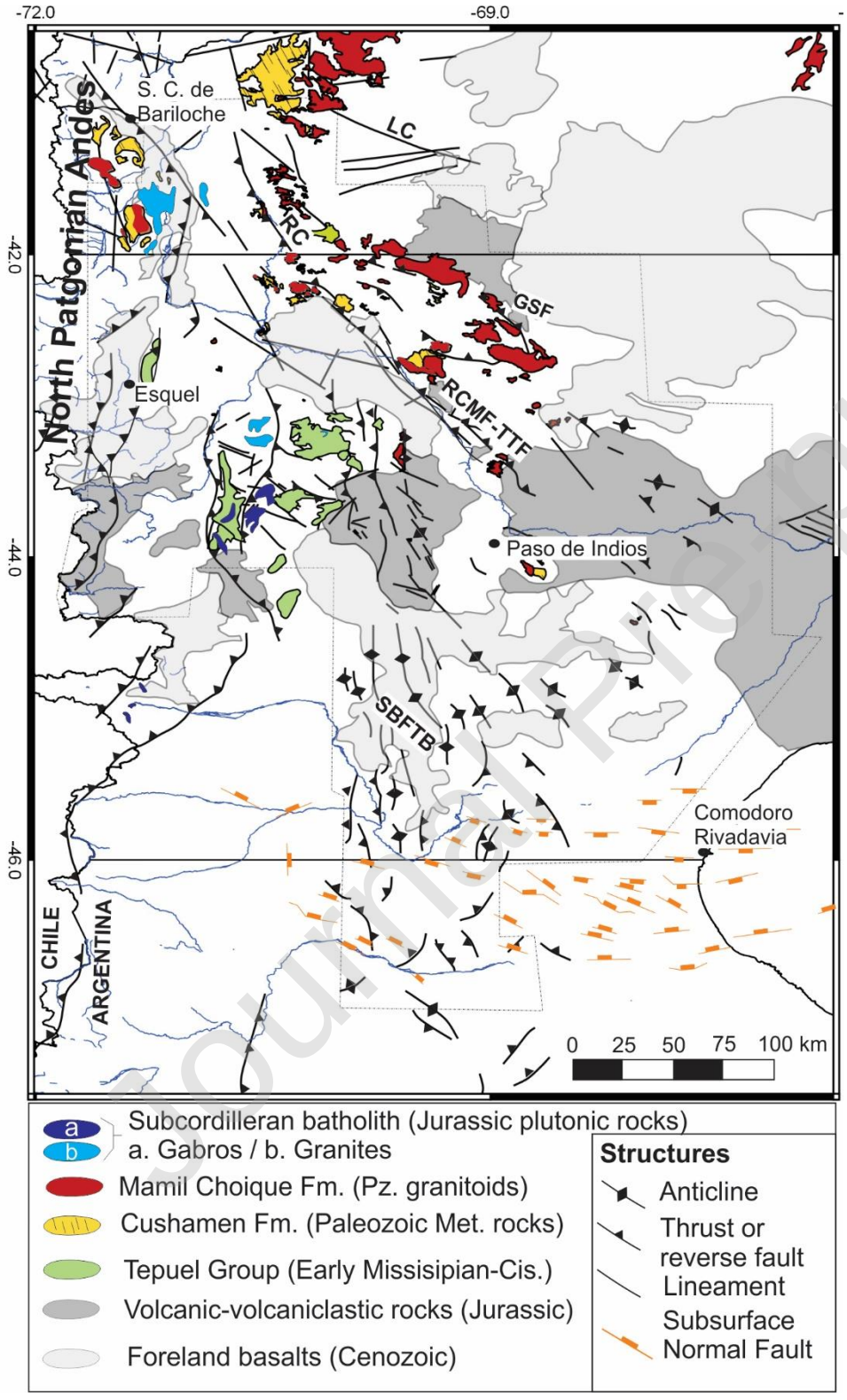

Figure 2. a) Structural map of the Patagonian foreland based on Dalla Salda & Franzese (1987); Giacosa et al. (2004), Bilmes et al. (2013), Gianni et al. (2015), Navarrete et al. (2016) and Echaurren et al. (2017). LC: Los Chilenos; RC: Río Chico; GSF: Gastre-Sacanana Fault; SN: Sierra Negra; RCMF-TTB: Río Chubut Medio Fault – Taquetrén Thrust Front; SBFTB: San Bernardo Fold and Thrust Belt

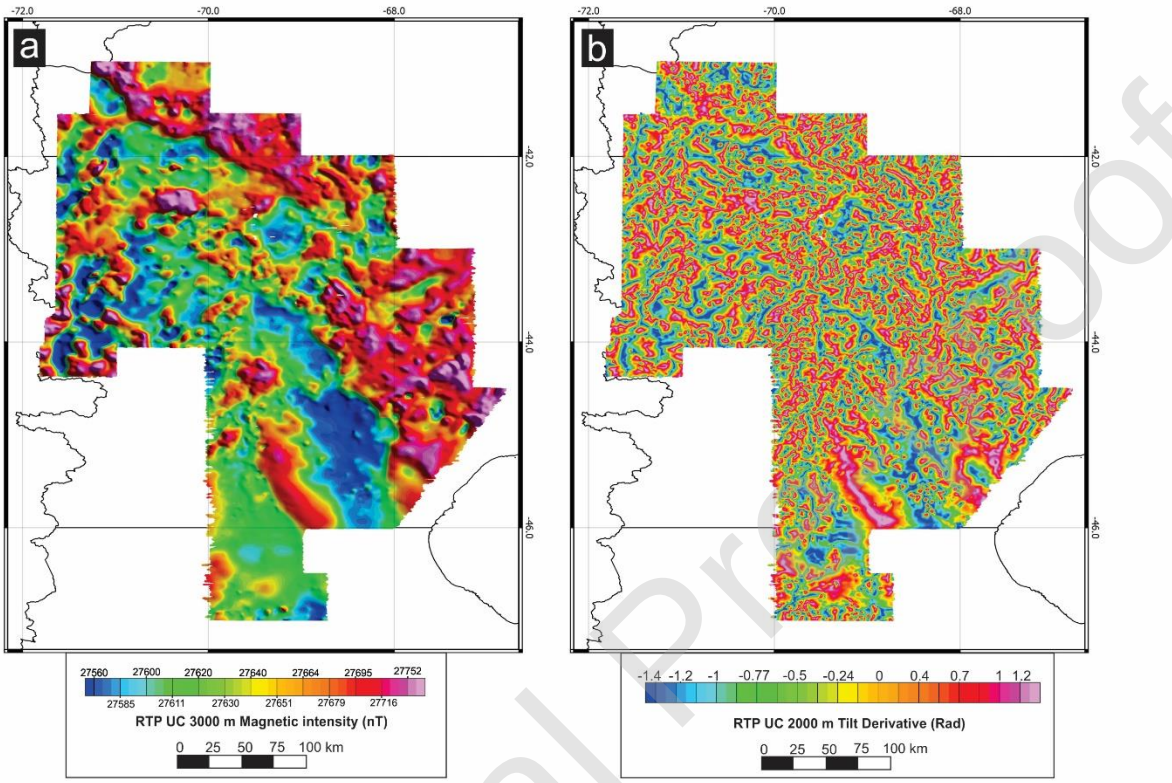
a
b
-72.0
-70.0
-68.0
-42.0
-44.0
-46.0
27560 27600 27620 27640 27664 27695 27752
27585 27611 27630 27651 27679 27716
RTP UC 3000 m Magnetic intensity (nT)
0 25 50 75 100 km
-1.4 -1.2 -1 -0.77 -0.5 -0.24 0 0.4 0.7 1 1.2
RTP UC 2000 m Tilt Derivative (Rad)

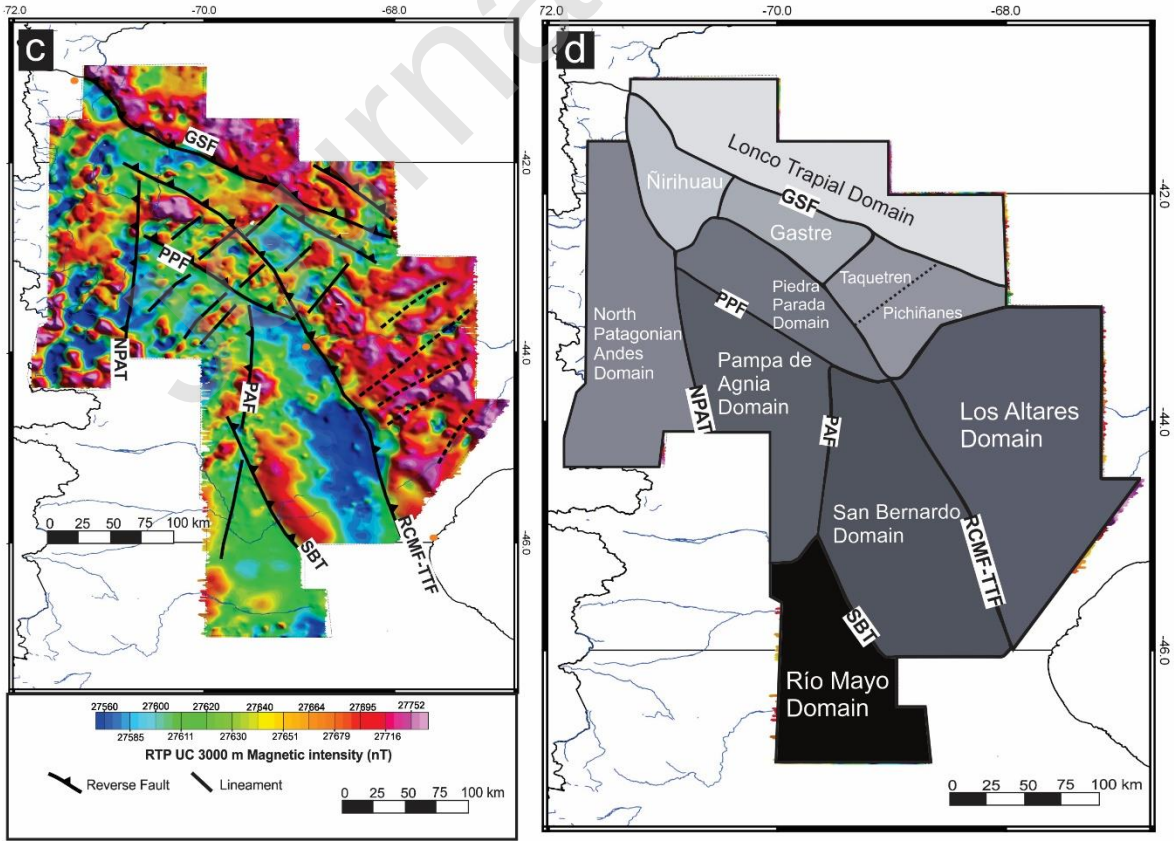
c
d
GSF
PPF
NPAT
PAF
SBT
RCMF-TTF
0 25 50 75 100 km
RTP UC 3000 m Magnetic intensity (nT)
Reverse Fault
Lineament
Lonco Trapial Domain
Nirihuau
Gastre
Taquetren
Piedra Parada Domain
Pichiñanes
North Patagonian Andes Domain
Pampa de Agnia Domain
Los Altares Domain
San Bernardo Domain
Río Mayo Domain

Figure 3. a) Coloured RTP aeromagnetic data upward continued to 3000 meters. b) Tilt derivative of the Reduced to pole Upward continued to 2000 meters data. c) Main regional structures are recognized. GSF: Gastre-Sacanana Fault; RCMF-TTF: Río Chubut Medio Fault – Taquetrén Thrust Front; SBT: San Bernardo Thrust; NPAT: North Patagonian Andes Thrust. PPF: Piedra Parada Fault, PAF: Pampa de Agnia Fault d) Structural Domains based on the RTP UC 3000 m map and contours defined by the RTP UC 2000 m TD.

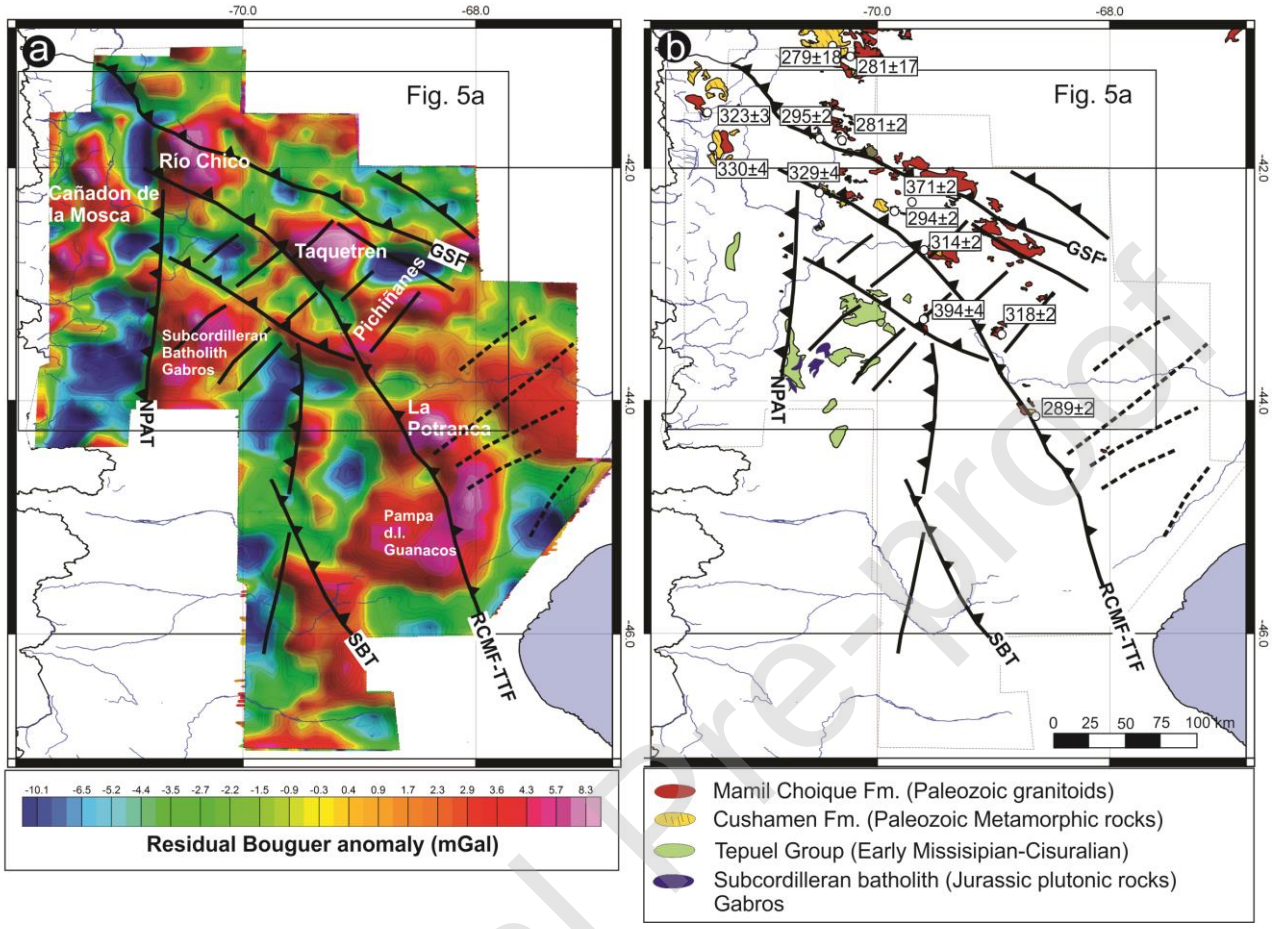

Figure 4. a) Composite image of the Residual Bouguer anomaly. Main structures interpreted from aeromagnetic data are shown. High-density crustal blocks are interpreted as Paleozoic basement igneous-metamorphic complexes. b) U-Pb zircon ages of Paleozoic igneous rocks exposed in the Patagonian foreland. Igneous complexes show a positive correlation with high amplitude gravimetric anomaly values. Ages from Pankhurst et al. (2006), data available in Table S2 (supplementary data)

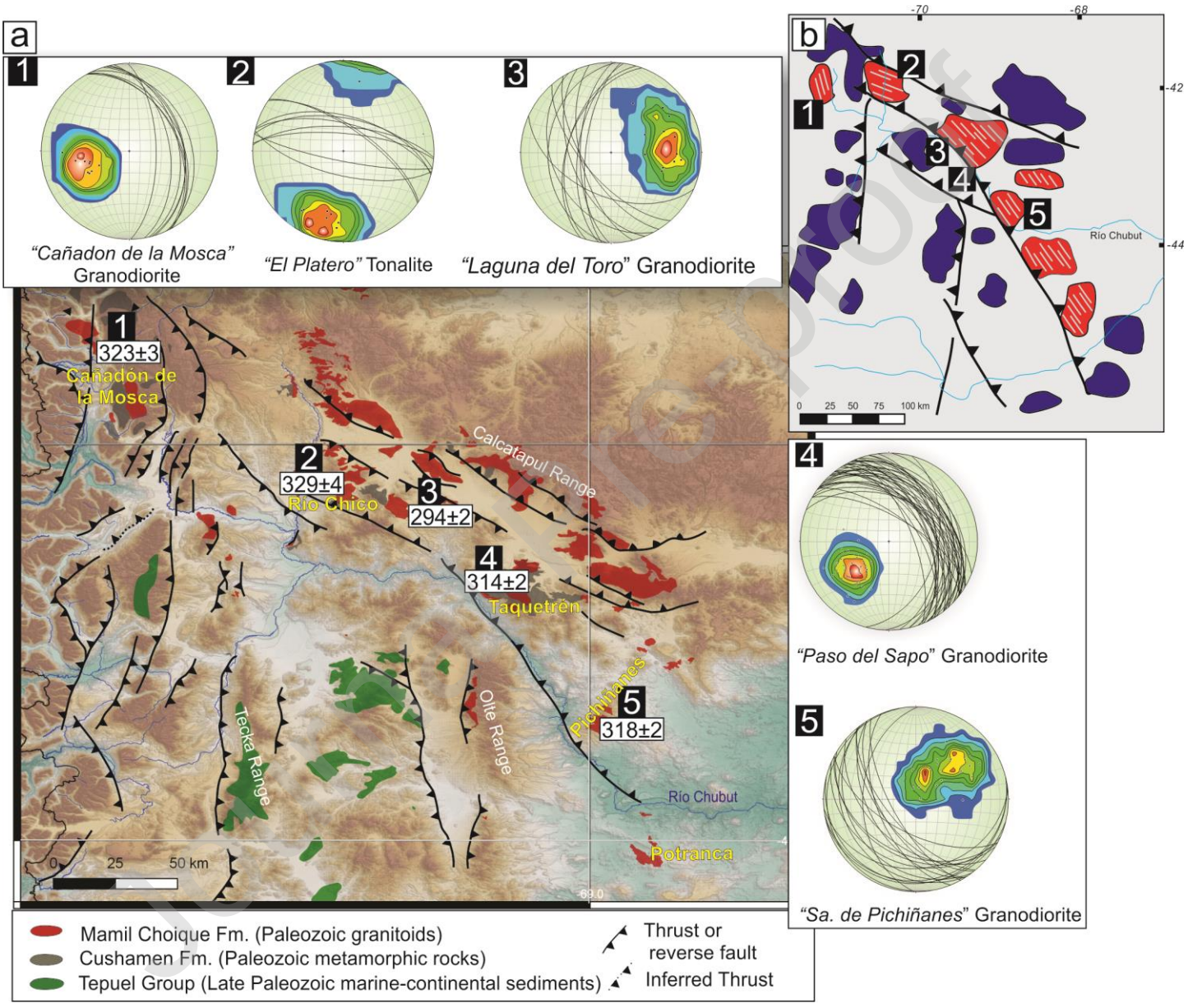
a
1
2
3
"Cañadon de la Mosca" Granodiorite
"El Platero" Tonalite
"Laguna del Toro" Granodiorite
1
323±3
Cañadón de la Mosca
2
329±4
Río Chico
3
294±2
4
314±2
Taquetrén
5
318±2
Calcatapul Range
Olte Range
Tecka Range
Pichiñanes
Río Chubut
Potranca
0 25 50 km
-69.0
b
-70
-68
-42
-44
Río Chubut
0 25 50 75 100 km
4
"Paso del Sapo" Granodiorite
5
"Sa. de Pichiñanes" Granodiorite
Mamil Choique Fm. (Paleozoic granitoids)
Cushamen Fm. (Paleozoic metamorphic rocks)
Tepuel Group (Late Paleozoic marine-continental sediments)
Thrust or reverse fault
Inferred Thrust

Figure 5. a) Internal structure of Late Paleozoic granitoids of the Patagonian broken foreland. Lower hemisphere equal area projections of poles and planes of magmatic foliations and layering (1 to 5). Localities in yellow refers to the crustal blocks defined in the Bouguer residual anomaly grid (Fig. 4a). b) High positive and high negative Bouguer anomaly values (red and blue respectively). High positive anomaly values are interpreted as generated by high-density basement blocks. The internal structure of this basement blocks is derived from a). U-Pb zircon ages of granitoids from Pankhurst et al. (2006) and available in table S2 (supplementary data).

Figure 6. Field photographs of solid-state (a) and magmatic structures (b to e). a) Mylonitic foliation in the Paso del Sapo mylonitic granite. b) Magmatic lineation defined by shape-preferred orientation of euhedral crystals of feldspar, hornblende and biotite in the Paso del Sapo

granodiorite. c) Preferred alignment of elongate enclaves parallel to magmatic foliation in the Laguna del Toro granodiorite. d) Magmatic foliation (S: 132°/48°W) defined by shape-preferred orientation of euhedral crystals of K-feldspar in the garnet-bearing Pichiñanes granite. e) Magmatic layering (299°/43°E) in the Cañadón de la Mosca intrusion.

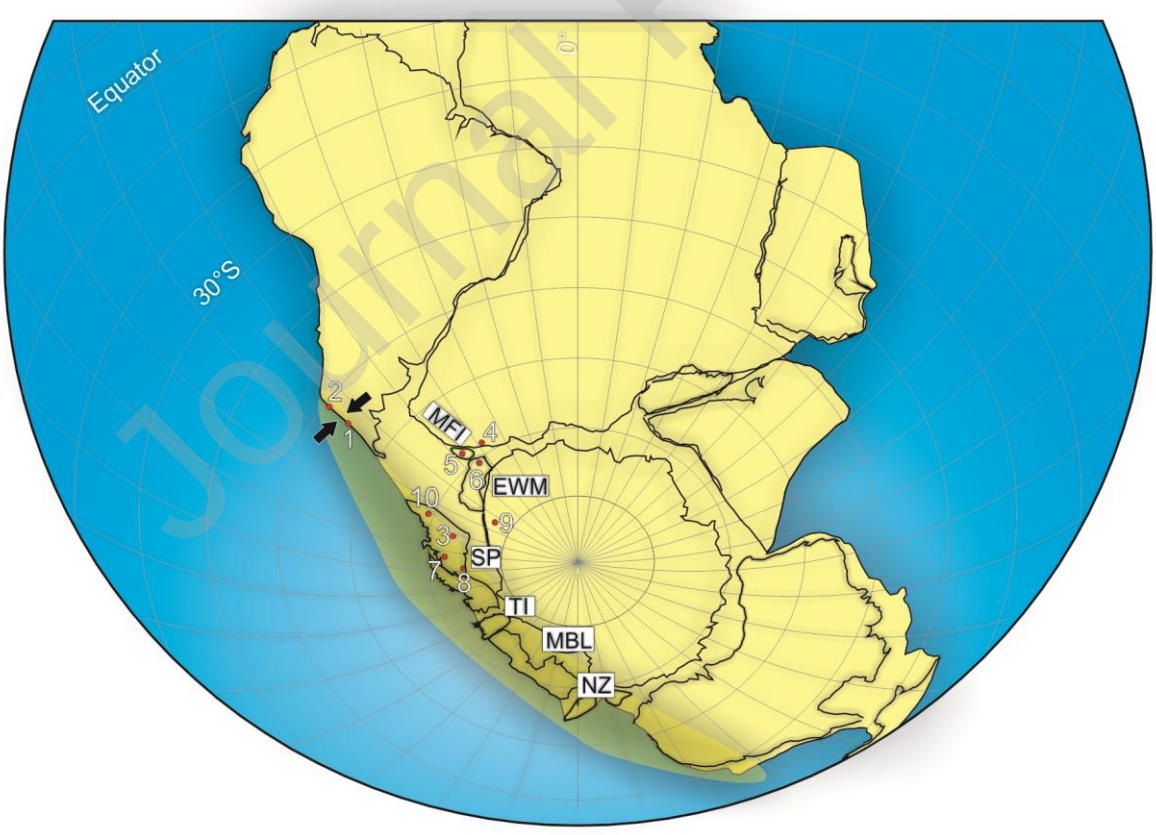

Figure 7. Absolute reconstruction of Gondwana for the Late Carboniferous (see text for for further explanations). SP (Southern Patagonia), MFI (Malvinas/Falkland Islands, Curtis and Hyam, 1998), EWM (Ellsworth Witmore Mountains block, Randall and Mac Niocaill, 2004; Jacobs and Thomas 2004), TI, MBL (Thurston Island and Marie Bird Land blocks, Elliot et al. 2016), NZ (New Zealand, Lawver and Scotese, 1987; Lacassie et al. 2006). 1: Taquetrén range, 2: Bariloche, 3: Don Camilo locality (Deseado Massif), 4: Durban (locality of a larger Natal-Namaqua belt), 5: Cape Meredith Complex (Natal-Namaqua belt), 6: outcrops of Natal-Namaqua belt in EWM, 7: Tres Lagos, 8: Pali Aike, 9: Shackleton range, 10: Tepuel-Genoa basin. Orientation of tectonic stress in northwestern Patagonia is indicated by black arrows. The shadowed yellow polygon represents the Southwestern Middle to Late Paleozoic Gondwanan active margin.

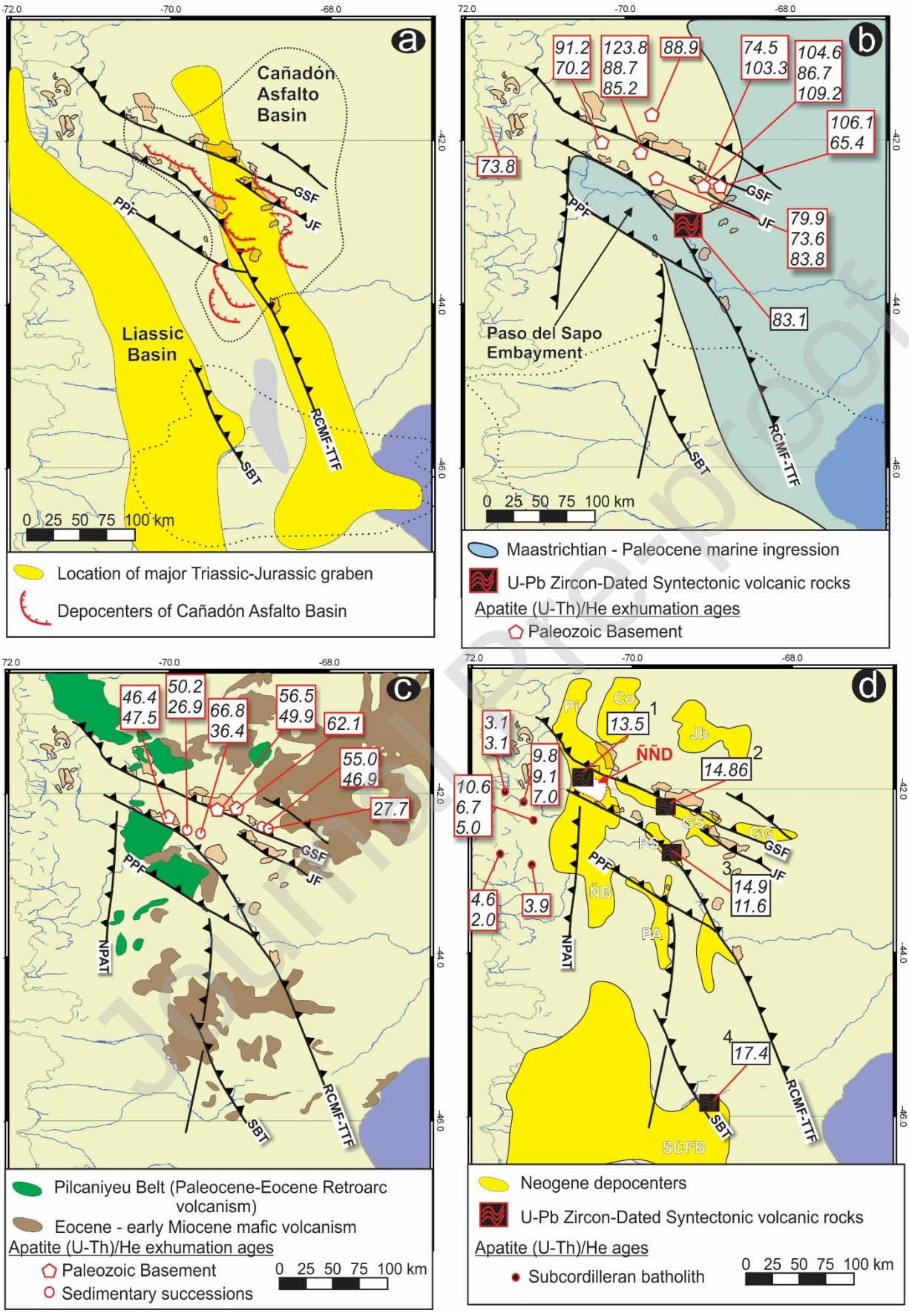

Figure 8. Regional structures for the Patagonian broken foreland and location of key units and structural elements for different periods. Paleozoic basement blocks are shown in light red. See text for discussion. a) Late Triassic - Early Jurassic location of graben systems, including depocenters of the Cañadón Asfalto Basin. In grey, subsurface Paleozoic basement from drilling cores are shown (based on Lesta et al., 1980; Linares and González, 1990; Uliana and Biddle., 1987; Figari et al., 2015). b) Late Cretaceous marine ingression after Scasso et al. (2012). Data from syntectonic volcanic U-Pb Zircon dated sequences (maximum deposition ages based on U-Pb detrital zircon data) (Echaurren et al., 2016), foreland Early-late/Late Cretaceous apatite (U-Th)/He exhumation ages of Paleozoic basement blocks (Savignano et al., 2016) and Late Cretaceous apatite (U-Th)/He exhumation ages from Andean ranges (Thomson et al., 2010) are also shown. c) Paleocene – Eocene retroarc volcanism (Pilcaniyeu belt) and Eocene – early Miocene mafic volcanism (adapted from Aragón et al., 2011; Ianelli et al., 2017; Fernández Paz et al., 2018) and its relationship with interpreted regional structures. Exhumation ages of Paleozoic basement blocks and Mesozoic sedimentary sequences from Savignano et al. (2016). d) Interpreted regional structures and location of Miocene foreland basins after Folguera and Ramos (2011), Bilmes et al. (2012, 2013) and Bucher et al. (2019). Apatite (U-Th)/He exhumation ages in Andean range from Savignano et al. (2016). Pi: Pilcaniyeu basin; ÑB: Ñorquinco Basin; SCFB: Santa Cruz Foreland Basin; PA: Pampa de Agnia Basin; PS: Paso del Sapo Basin; GS: Gastre Basin; GG: Gan Gan Basin; Jb: Jacobacci Basin; Co: Comallo Basin. Foreland syntectonic volcanic U-Pb Zircon ages from 1. Ramos et al. (2015), 2. Bilmes et al. (2013), 3. Bucher et al. (2019), 4. Gianni et al. (2017). All data is available in the supplementary material (Table S2).